

AMERICAN UNIVERSITY OF BEIRUT

METEOROLOGICAL SIMULATIONS TO INVESTIGATE THE
STRATEGIES IN MITIGATING URBAN HEAT ISLAND (UHI)
EFFECT IN A NEIGHBORHOOD IN BEIRUT CITY:
A MODEL BASED APPROACH

by
HASAN JAAFAR

A thesis
submitted in partial fulfillment of the requirements
for the degree of Master of Engineering
to the Department of Mechanical Engineering
of the Maroun Semaan Faculty of Engineering and Architecture
at the American University of Beirut

Beirut, Lebanon
June 2020

AMERICAN UNIVERSITY OF BEIRUT

METEOROLOGICAL SIMULATIONS TO INVESTIGATE THE STRATEGIES IN MITIGATING URBAN HEAT ISLAND (UHI) EFFECT IN A NEIGHBORHOOD IN BEIRUT CITY:
A MODEL BASED APPROACH

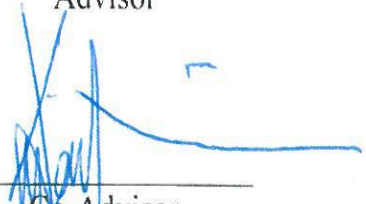
by
HASAN JAAFAR

Approved by:

Dr. Issam Lakkis, Chairperson & Professor
Department of Mechanical Engineering


Advisor

Aram Yeretzian, Assistant Professor
Department of Architecture and Design


Co-Advisor

Dr. Kamel Aboughali, Professor
Department of Mechanical Engineering


Member of Committee

Dr. Sara Najem, Assistant Professor
Department of Physics


Sara Najem (Lent 26, 2020 18:18 GMT+3)

Member of Committee

Date of thesis/dissertation defense: June 18, 2020

AMERICAN UNIVERSITY OF BEIRUT

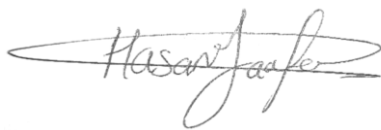
THESIS, DISSERTATION, PROJECT RELEASE FORM

Student Name: Jaafar Hasan Ali
Last First Middle

Master's Thesis Master's Project Doctoral Dissertation

I authorize the American University of Beirut to: (a) reproduce hard or electronic copies of my thesis, dissertation, or project; (b) include such copies in the archives and digital repositories of the University; and (c) make freely available such copies to third parties for research or educational purposes.

I authorize the American University of Beirut, to: (a) reproduce hard or electronic copies of it; (b) include such copies in the archives and digital repositories of the University; and (c) make freely available such copies to third parties for research or educational purposes after: **One** ---- year from the date of submission of my thesis, dissertation, or project.
Two ---- years from the date of submission of my thesis, dissertation, or project.
Three ---- years from the date of submission of my thesis, dissertation, or project.



03/July/2020

Signature

Date

This form is signed when submitting the thesis, dissertation, or project to the University Libraries

ACKNOWLEDGMENTS

I would like to express my sincere gratitude to my professors and supervisors Dr. Issam Lakkis and Dr. Aram Yeretian for all the help, support, patience, and guidance throughout the thesis process. Thank you for the research experience you made me have and for allowing me the opportunity to realize my goals.

To my committee members, Prof Dr. Kamel Abou Ghali and Dr. Sara Najem, I would like to express my greatest appreciation for their valuable feedbacks that indirectly helped me accomplish this work.

I would like also to express my gratitude to all my friends for their encouragement and special thanks to all my lab mates and colleagues for making my experience more entertaining and for their elevating inspiration. The research could not have been accomplished without their support.

Last, but not least, my parents are also an important inspiration for me and for being by my side when the times got rough. Thank you for believing in me.

AN ABSTRACT OF THE THESIS OF

Hasan Jaafar for

Master of Engineering
Major: Applied Energy

Title: Meteorological Simulations to Investigate the Strategies in Mitigating Urban Heat Island (UHI) Effect in a Neighborhood in Beirut City: A Model Based Approach

The Urban heat island (UHI) effect is a threatening event expected to be as alarming as global warming. Given the aforementioned, several mitigation strategies were investigated in order to detect which has the most impact on alleviating the UHI effect in a neighborhood in Beirut city, the capital of Lebanon. These include changing the ground surface albedo, replacing old buildings with new ones, and last but not least adding vegetation. This was simulated through use of ENVI-met V4.4 software.

The simulations were conducted on the 20th of January and August to exploit two main seasons in the country, which are winter and summer seasons, respectively. The simulations were carried on a 200 x 200 x 46-meter domain at a resolution of 2 meters, which enables the study of small-scale interfaces between buildings, surfaces, and vegetation. The present study will allow urban planners to determine the precise policies needed to meliorate the urban living environment in cities in parallel with Beirut.

Furthermore, the simulation which exhibited the most impact in reducing UHI effect is the including of vegetation. It demonstrated to be the most effective mitigation strategy given its ability to improve the thermal comfort conditions at the pedestrian's pathway sidewalks. The maximum decrease in air temperature was 2.4°C at 17:00 on August 20th, while the maximum decrease in the mean radiant temperature was 10.5°C at 12 noon. Besides, the optimum cooling regarding the outdoor thermal comfort (PET) was recorded in street S2 with an average reduction by 3.8°C. In addition, another study was conducted to examine the effects of climate change on Beirut for more accurate forecasts and unerring precautions.

CONTENTS

ACKNOWLEDGMENTS	V
ABSTRACT	VI
LIST OF ILLUSTRATIONS	IX
LIST OF TABLES.....	XI

Chapter

1. INTRODUCTION	1
1.1. Thesis Topic Definition	1
1.2. Aim and Research Objectives	2
2. LITERATURE REVIEW	3
2.1. Factors influencing UHI effect.....	3
2.2. Albedo.....	3
2.3. Vegetation	4
2.4. Urban Geometry.....	5
2.5. Assessing Environmental Factors	6
2.5.1. Air Temperature.....	6
2.5.2. Wind Speed.....	6
2.5.3. Relative Humidity.....	6
2.5.4. Mean Radiant Temperature.....	7
2.6. Previous Studies	7
3. METHODOLOGY.....	10
3.1. Case Study Selection and Description	10
3.2. Control Variables	14
3.3. Base Case Scenario	15
3.3.1. Input Parameters.....	17
3.4. Proposed Scenarios	18
3.5. Outdoor Thermal Comfort	20
3.6. Climate Change and Future Prediction	22

4. LATERAL BOUNDARY CONDITIONS AND NESTING CELLS.....	24
4.1. Lateral Boundary Condition.....	24
4.2. Nesting Cells.....	26
5. RESULTS	28
5.1. Model Validation using L2 Norm Method.....	28
5.2. Air Temperature.....	30
5.3. Wind Speed.....	32
5.4. Relative Humidity.....	34
5.5. Mean Radiant Temperature.....	36
5.6. Ground Surface Temperature.....	39
5.7. Outdoor Thermal Comfort	41
6. DISCUSSION	44
7. CONCLUSION	46
 BIBLIOGRAPHY	 48

ILLUSTRATIONS

Figure	Page
1. Urban Heat Island Effect between the City and its Surrounding (O'Malley, C., Piroozfar, P., Farr, E. R., & Pomponi, F. , 2015)	1
2. Radiative Properties of Natural Materials (Oke, T. R. , 2002).	4
3. Evapotranspiration Process (Evapotranspiration: The Oft-Forgotten Outflow, 2012).	5
4. Geographic Location of Beirut and the Studied Area (Google Earth, 2017).	11
5. Flow Chart of the Study Methodology.	13
6. 3D Model Area by ENVI-met.	17
7. Pedestrian sidewalk illustrated on the base case scenario.	18
8. First scenario, replacing asphalt cover with cool pavement. (Heat Island, n.d.)	19
9. Second scenario with 25% vegetation added to the base case.	20
10. Third scenario where blue colored old buildings were replaced with new ones.	20
11. Base case scenario with S1 and S2 streets.	21
12. Input file drawing for ENVI-met simulations.	25
Figure 13. Air temperature comparison between Reference and other cases using L2 norm error method.	29
14. Wind speed comparison between Reference and other cases using L2 norm error method.	29
15. Comparison of hourly average air temperature results for different scenarios on August 20 th	30
16. Comparison of hourly average air temperature results for different scenarios on January 20 th	31
17. Absolute difference in air temperature between various heat mitigation scenarios and the base case scenario at 12:00 at 1.4m elevation from ground level.	32
18. Comparison of hourly average wind speed results for different scenarios on August 20 th	33
19. Comparison of hourly average wind speed results for different scenarios on January 20 th	33
20. Absolute difference in wind speed between various heat mitigation scenarios and the base case scenario at 12:00 at 1.4m elevation from ground level.	34
21. Comparison of hourly average relative humidity results for different scenarios on August 20 th	35
22. Comparison of hourly average relative humidity results for different scenarios on January 20 th	35
23. Absolute difference in relative humidity between various heat mitigation scenarios and the base case scenario at 12:00 at 1.4m elevation from ground level.	36
24. Comparison of hourly average mean radiant temperature results for different scenarios on August 20 th	37
25. Comparison of hourly average mean radiant temperature results for different scenarios on January 20 th	38

26. Absolute difference in mean radiant temperature between various heat mitigation scenarios and the base case scenario at 12:00 at 1.4m elevation from ground level.	39
27. Comparison of hourly average ground surface temperature results for different scenarios on August 20 th	40
28. Comparison of hourly average ground surface temperature results for different scenarios on January 20 th	40
29. Absolute difference in ground surface temperature between various heat mitigation scenarios and the base case scenario at 12:00 at the ground level.	41
30. PET change at 1.4m above the ground level on a typical summer day (20 th August) at two locations with the base case scenario and the vegetation scenario.	42
31. PET simulation for both scenarios at three different hours.	43

TABLES

Table	Page
1. Controlled variables with their assessment criteria.	14
2. Type and total number of trees in the studied area.	16
3. Thermal characteristics for building materials.	16
4. Model configuration and initialization parameters for the simulations.	17
5. Road characteristics for the simulations.	17
6. Proposed scenarios with their controlled variables.	19
7. Setting for PET Calculation.	22
8. Thermal sensation according to PMV and PET values.	22
9. Different model areas with different numbers of nesting cells.	27

CHAPTER 1

INTRODUCTION

1.1 Thesis Topic Definition

Urban areas contain over half the world's population (Jansson, Å, 2013), and are responsible for increasing the world's energy consumption by up to 80% (Kamal-Chaoui, L., & Robert, A., 2009). Urban heat island (UHI) is a major problem in urban cities around the world. The term urban heat island, is recognized as an international threat of the 21st century (Gasparrini, A., Guo, Y., Sera, F., Vicedo-Cabrera, A. M., Huber, V., Tong, S., ... & Ortega, N. V., 2017), refers to higher urban temperatures in city centers (Figure 1) compared to the suburban or surrounding rural areas (Santamouris, M, 2013). One of the main differences between rural and urban areas is that rural areas contain many open spaces and large vegetated surfaces that result in lower and cooler temperatures. Due to rapid urbanization, many cities are now crowded and overpopulated leading to several environmental issues such as pollution and urban heat island.

This phenomenon results from the density of buildings that are characterized by low albedo and high thermal energy storage capacity, in addition to the depletion green spaces and the production of anthropogenic heat (Santamouris, M., Synnefa, A., & Karlessi, T., 2011).

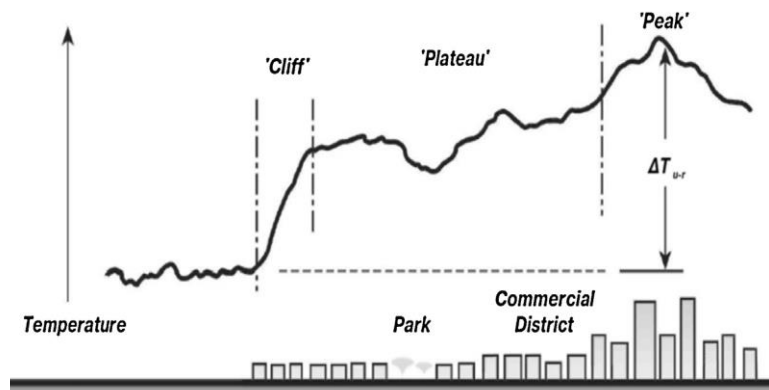


Figure 1. Urban Heat Island Effect between the City and its Surrounding (O'Malley, C., Piroozfar, P., Farr, E. R., & Pomponi, F., 2015).

1.2 Aim and Research Objectives

The aim of this research is to investigate the influence of different heat mitigation strategies on the microclimate of a neighborhood in Beirut city called Hamra. Moreover, the aim is to propose solutions that would help induce the minimization impacts of the UHI which will lead to the improvement in the overall living conditions.

In evaluating different strategies and identifying the most efficient one, microclimate models can be of great use. Microclimate models such as RayMan and ENVI-met are tools that can be used to predict climatic features of the urban environment and can be important in assessing the relationship between the climate and the urban modification scenarios. Also, these models can be used to evaluate any urban configuration scenario and to answer specific questions relating to design and urban planning. Many variables that affect the urban heat island effect were investigated, such as adding vegetation, replacing old buildings with new ones, and modifying the albedo of the ground cover.

The main objectives of this research are:

1. To predict the way the meteorological conditions will be influenced with the use of UHI mitigation strategies, in Beirut.
2. To understand the effect of the controlled variables on the outdoor meteorological conditions.
3. To show the importance of the lateral boundary conditions and the effect of adding periphery buildings on the results.
4. To examine the effect of climate change on Beirut for accurate forecasts and unerring precautions.

CHAPTER 2

LITERATURE REVIEW

This section covers the factors that influence the UHI phenomenon and what are the strategies to mitigate this effect.

2.1 Factors influencing UHI effect

Meteorological and urban factors together cause an increase in the air temperature in urban cities. This increase in the air temperature of the city will reduce the human thermal comfort leading people to stay inside their homes and will increase the energy consumption for cooling purposes (Weng, Q. , 2001). Meteorological factors are natural factors such as temperature, wind speed and direction, radiation, and cloud covers, while urban geometry plays a vital role in the UHI since dense and high urban geometry will block the solar radiation from coming in; also, it will reduce the wind speed.

Whereas anthropogenic heat results from general human activities such as car emissions, use of generators, air conditioning, and industrial facilities that have a significant impact on the environment (Che-Ani, A. I., Shahmohamadi, P., Sairi, A., Mohd-Nor, M. F. I., Zain, M. F. M., & Surat, M., 2009).

2.2 Albedo

UHI phenomenon can be affected by the type of material used and its albedo property.

Albedo properties that are listed in the figure below (figure 2), is the ratio or proportion of light or radiation that is reflected into the atmosphere by a surface. For example, low albedo materials mean that the surface reflects small amount of the radiation and absorbs the rest.

Man-made structures mainly have a low albedo. This means that the low amount of energy is reflected by the surface causing increase in the surrounding air temperature due to the heat absorbed and stored, which came from the sun. Cities are usually composed of medium and

tall buildings that have a diversity of materials that vary from light to dark concrete surfaces and low albedo values. Building materials have been found to have an important effect on the urban microclimate. By changing the materials of the buildings, the amount of direct and diffused solar radiation that are getting into the space can be better controlled. Building materials affect the microclimate by absorbing heat during the day and releasing it back to the atmosphere at night (Asaeda, A., Ca, V.T., Akio Wake, A., 1994). For the roads and streets in the cities, concrete and asphalt are being used that are replacing the vegetative surfaces. These roads and streets are made of low albedo properties with high storage capacities which increase the urban temperature. Converting natural land covers into asphalt or concrete cause higher air and surface ground temperature compared to rural areas (Gartland, L. M. , 2012).

Surface	Remarks	Albedo α	Emissivity ϵ
Soils	Dark, wet	0.05–	0.98–
	Light, dry	0.40	0.90
Desert		0.20–0.45	0.84–0.91
Grass	Long (1.0 m)	0.16–	0.90–
	Short (0.02 m)	0.26	0.95
Agricultural crops, tundra		0.18–0.25	0.90–0.99
Orchards		0.15–0.20	
Forests			
	Deciduous	Bare	0.15–
	Leaved	0.20	0.98
	Coniferous	0.05–0.15	0.97–0.99
Water	Small zenith angle	0.03–0.10	0.92–0.97
	Large zenith angle	0.10–1.00	0.92–0.97
Snow	Old	0.40–	0.82–
	Fresh	0.95	0.99
Ice	Sea	0.30–0.45	0.92–0.97
	Glacier	0.20–0.40	

Figure 2. Radiative Properties of Natural Materials (Oke, T. R. , 2002).

2.3 Vegetation

The absence of trees impacts the UHI in many ways since the trees will prevent solar energy from reaching the below surfaces, thus maintaining lower temperatures. Solar radiation is one of the main heat sources in the buildings. Therefore, combining the vegetation with the building surfaces will be a helpful way of controlling the heat gain coming from solar radiation (Peri, G., Rizzo, G., Scaccianoce, G., La Gennusa, M., & Jones, P. , 2016). As urbanization continues to expand, more vegetation will be lost, thus increasing the urban

temperature. On the other hand, the trees are responsible for increasing the latent heat exchange through evaporative cooling by a process called evapotranspiration (figure 3), making the air temperature cooler (Grimmond, C. S. B., & Oke, T. R. , 1991). According to a study, the evapotranspiration under optimal conditions can cool the air temperature by 2 to 8°C around surrounding areas and green spaces (Akbari, H., Pomerantz, M., Taha, H., 2001). Vegetation also provides other benefits in urban areas such as improving air quality (O₂), reducing energy demand for air conditioning, and for the soil erosion control.

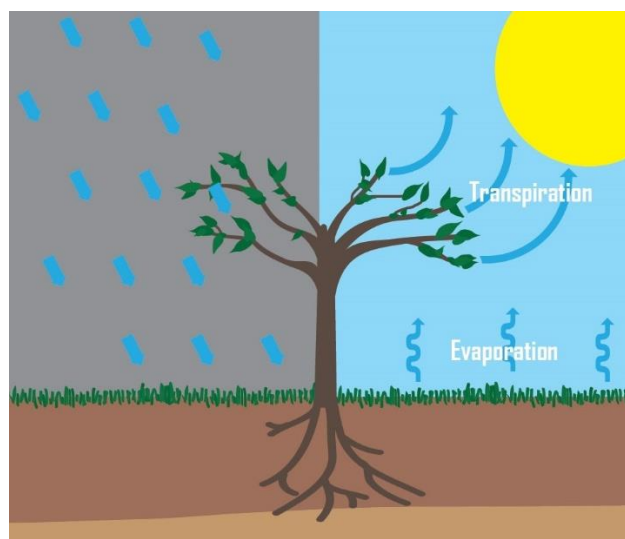


Figure 3. Evapotranspiration Process (*Evapotranspiration: The Oft-Forgotten Outflow*, 2012).

2.4 Urban Geometry

Urban geometry directly affects the following parameters such as solar radiation, wind speed, air temperature, and thermal comfort of the pedestrian because the change in the sky view factor (SKV), the height to width ratio (H/W) of the street canyons, and the orientation for the street canyons. . In an urban area with high sky view factor, the air temperature was higher in the daytime due to the high heat capacity of urban materials in open spaces (Wang, Y., & Akbari, H. , 2016).

2.5 Assessing Environmental Factors

2.5.1 Air Temperature

Air temperature is mainly used to evaluate the temperature distribution due to building arrangements as well as the material properties of the building enclosure and the ground. Canyons, where the street is sided by buildings on both sides, with a different orientation do not vary among sites and do not affect air temperature (Chatzidimitriou, A., & Axarli, K. , 2017). An experimental study developed a correlation between the air temperature compared to solar radiation and found that a change in 59 W/m^2 in solar radiation will lead to change of 1°C in air temperature (Givoni, B., Noguchi, M., Saaroni, H., Pochter, O., Yaacov, Y., Feller, N., & Becker, S., 2003).

2.5.2 Wind Speed

Wind velocity is used to evaluate the air movement distribution in the urban canopy (the space between buildings and under the street roofs). Wind speed influences convection and evaporation. The orientation of the canyons plays an important role in the distribution of the wind speed. Also, during the winter season, the wind speed may create discomfort due to the high wind speed, which makes it hard for the pedestrian to move outdoor. This results in uncomfortable outdoor environments (Gaspari, J., & Fabbri, K. , 2017).

2.5.3 Relative Humidity

Relative humidity, measured in %, is used to evaluate the effect of the vegetation. Also, the value of the relative humidity has a direct influence on the latent load, thus on human sweating. Relative humidity, which is higher than 65% during the summer season, is identified as discomfort, due to the warm and humid weather (Gaspari, J., & Fabbri, K. , 2017).

2.5.4 Mean Radiant Temperature

Mean radiant temperature (T_{mrt}) is defined according to ASHRAE as ‘uniform temperature of an imaginary enclosure in which the radiant heat transfer from the human body equals the radiant heat transfer in the actual non-uniform enclosure.’ Mean radiant temperature is an important variable that affects the outdoor thermal comfort of the human (Lindberg, F., Holmer, B., & Thorsson, S. , 2008). Outdoor spaces such as the public open spaces or where the pedestrian walk is mainly affected by the direct solar radiation and the surface temperature of the suburban elements (building materials, street pavements, etc.), which will lead to the increase in the mean radiant temperature. Several strategies were implemented to decrease the mean radiant temperature, such as adding trees that will form shades. A study revealed that adding extra trees in a park will form a cooling effect for the pedestrian by decreasing the air temperature and the mean radiant temperature (Nasir, R. A., Ahmad, S. S., Zain-Ahmed, A., & Ibrahim, N. , 2015).

2.6 Previous Studies

Several studies have been devoted in understanding the intensities of UHI effects in large and medium sized cities. A study in Athens showed that the highest temperatures were recorded in the afternoon hours (Kourtidis, K., Georgoulas, A. K., Rapsomanikis, S., Amiridis, V., Keramitsoglou, I., Hooyberghs, H., ... & Melas, D. , 2015). Moreover, it showed that an increase in the urbanization and anthropogenic heat play a vital role in increasing the urban temperature. In addition, an increase in urban heat islands also indicated a correlation between the growth of the urban city and the UHI effect (Giannopoulou, K., Livada, I., Santamouris, M., Saliari, M., Assimakopoulos, M., & Caouris, Y. G. , 2011). Another study conducted in Spain, in the city of Salamanca, compared the temperature in an urban area to a nearby rural area and found that the UHI is more critical during the night-time (Alonso, M. S., Labajo, J. L., & Fidalgo, M. R. , 2003). Another study found that the light-colored

surfaces are cooler than the dark ones when tested on paving materials of different colors and areas with different albedo values and thermal properties (Doulos, L., Santamouris, M., & Livada, I. , 2004). In another study, 14 types of reflective coatings were investigated, such as building walls and roofs, sidewalks, and pavements, and found that the use of reflective coating with high solar reflectance properties can reduce the surface temperature (Synnefa, A., Santamouris, M., & Livada, I. , 2006). Several researchers suggested that urban surfaces should have high albedo properties whenever possible (Synnefa, A., Dandou, A., Santamouris, M., Tombrou, M., & Soulakellis, N. , 2008; Santamouris, M., Gaitani, N., Spanou, A., Saliari, M., Giannopoulou, K., Vasilakopoulou, K., & Kardomateas, T. , 2012). Cooling the roof surfaces will lead to a decrease in their temperature and could contribute to UHI mitigation, which would result in the reduction of the indoor air temperature and lower the cooling energy demand (Zinzi, M., & Agnoli, S. , 2012). A study showed that the presence of vegetation lowered both the surface temperature and the air temperature near the surface because of the evapotranspiration and the shading (Loughner, C. P., Allen, D. J., Zhang, D. L., Pickering, K. E., Dickerson, R. R., & Landry, L. , 2012). Increasing the number of shade trees in urban canyons has an important role in enhancing the thermal comfort levels of the urban streets (Ali-Toudert, F., & Mayer, H. , 2006).

Therefore, the measures to mitigate UHI effects are, shading of urban areas by trees (Takebayashi, H., & Moriyama, M. , 2012), using cool materials for streets and pavement covers (Dimoudi, A., Zoras, S., Kantzioura, A., Stogiannou, X., Kosmopoulos, P., & Pallas, C. , 2014), green spaces such as urban gardens or parks that are known to provide a good solution to the urban heat stress (Santamouris, M. , 2014), and presence of urban water bodies such as rivers or lakes (Kleerekoper, L., Van Esch, M., & Salcedo, T. B. , 2012).

Moreover, UHI is mainly known as a phenomenon of climate change, which can affect the health of human beings directly due to the increase in the outdoor temperature (Gasparrini,

A., Guo, Y., Sera, F., Vicedo-Cabrera, A. M., Huber, V., Tong, S., ... & Ortega, N. V. , 2017). Climate change risk can be reduced by mitigation strategies, and without these strategies, a study predicts an increase in the surface temperature between 2.6°C and 4.8°C by the end of 2100 (Pachauri, R. K., Allen, M. R., Barros, V. R., Broome, J., Cramer, W., Christ, R., ... & Dubash, N. K. , 2014). Therefore, urban climate research should take into consideration the rapid urban growth that is occurring.

CHAPTER 3

METHODOLOGY

As for the methodology, an investigation was performed on the parameters that are responsible for the UHI effect in Beirut. Moreover, an analysis was conducted to verify which mitigate strategy is optimal in reducing the UHI effect, in addition to study the outdoor thermal comfort on the pedestrian.

3.1 Case Study Selection and Description

In the Middle East, Lebanon is a small country located on the eastern coast of the Mediterranean Sea, with a surface area of 10,452 km² and a total population of 5,988,000 (UN 2015 United Nation Population Division, 2015). Recent data shows that 87.8% of this population lives in urban areas (UN 2015 United Nation Population Division, 2015). Beirut, the capital city of Lebanon, which covers 21.47 km², with latitude 33.88 and longitude 35.49, was chosen in which the study will be conducted in one of its neighborhoods. In Beirut, the urban vegetation covers only 21% of its total urban surface area, while asphalt and basalt roads cover as much as 25% of its urban surface area (Kaloustian, N., & Diab, Y. , 2015). This city belongs to the Csa category of Köppen's climate classification (Köppen, W. , 1990), whereby its climate is characterized by a hot, humid summer and a mild winter. Figure 4 shows the selected case study in the Hamra area. This area was selected due to the design of the streets, the variability in heights of the buildings (mid-rise and low-rise buildings), and the lack of vegetation.



Figure 4. Geographic Location of Beirut and the Studied Area (*Google Earth, 2017*).

In this research, the aim is to examine the effect of heat mitigation strategies on pedestrian thermal comfort in Hamra neighborhood. The following section describes the controlled variables that will be used, the base case scenario and the proposed scenarios.

The flowchart (figure 5) presents the methodology and the process of the study. In the beginning, the site and location were selected. Due to limited data being available regarding the existing old buildings present in Beirut, the most suitable way to control the buildings being tested on is relying on the age of the buildings. Buildings before 1995 will be defined as old buildings with single walls and single glazing, while buildings after the year 1995 (new buildings) will have double walls and double glazing. As a result, we can identify the materials used for construction purposes at each period. Also, a survey was conducted in the area to calculate the windows to wall ratio (WWR) on each façade of the buildings which was needed for the model on ENVI-met. After finishing the base case model, the simulation was run for 24 hours on two chosen dates, one on a summer day (20th August) and the other on a winter day (20th January). The base case model was tested several times for calibration and for selecting the best number of nesting cells using the L2 norm method. The L2 norm (Euclidean norm) error is a method that was used for the comparison among the cases due to

lack of field measurement. L2 norm is used to calculate the distance of the vector coordinates from the origin of the vector space. This method helps calculate and estimate the errors between any two cases.

$$L2 \text{ Norm Error Percentage} = \frac{\sqrt{(\sum_{i=1}^{\infty} \|(X_i - X_i^*)\|^2)}}{\sqrt{(\sum_{i=1}^{\infty} \|(X_i)\|^2)}} \times 100$$

Where: X_i^* referred to the current value, and X_i referred to the reference case value.

Several scenarios will be proposed and simulated, including climate change and future prediction for Beirut city. The proposed scenarios will be simulated for a 24 hours span taking into account variables such as air temperature, wind speed, relative humidity, mean radiant temperature and ground surface temperature to compare between the base case scenario and the proposed one.

The analysis of the results was based on the pedestrian path sidewalk near the buildings at an elevation of 1.4 m from ground level, as shown in figure 7, to check how these variables would be affected after the mitigation scenarios were implemented. Therefore, the results compared the average hourly data of the pedestrian sidewalk between the base case and the proposed scenarios in addition to the absolute difference at 12:00 PM.

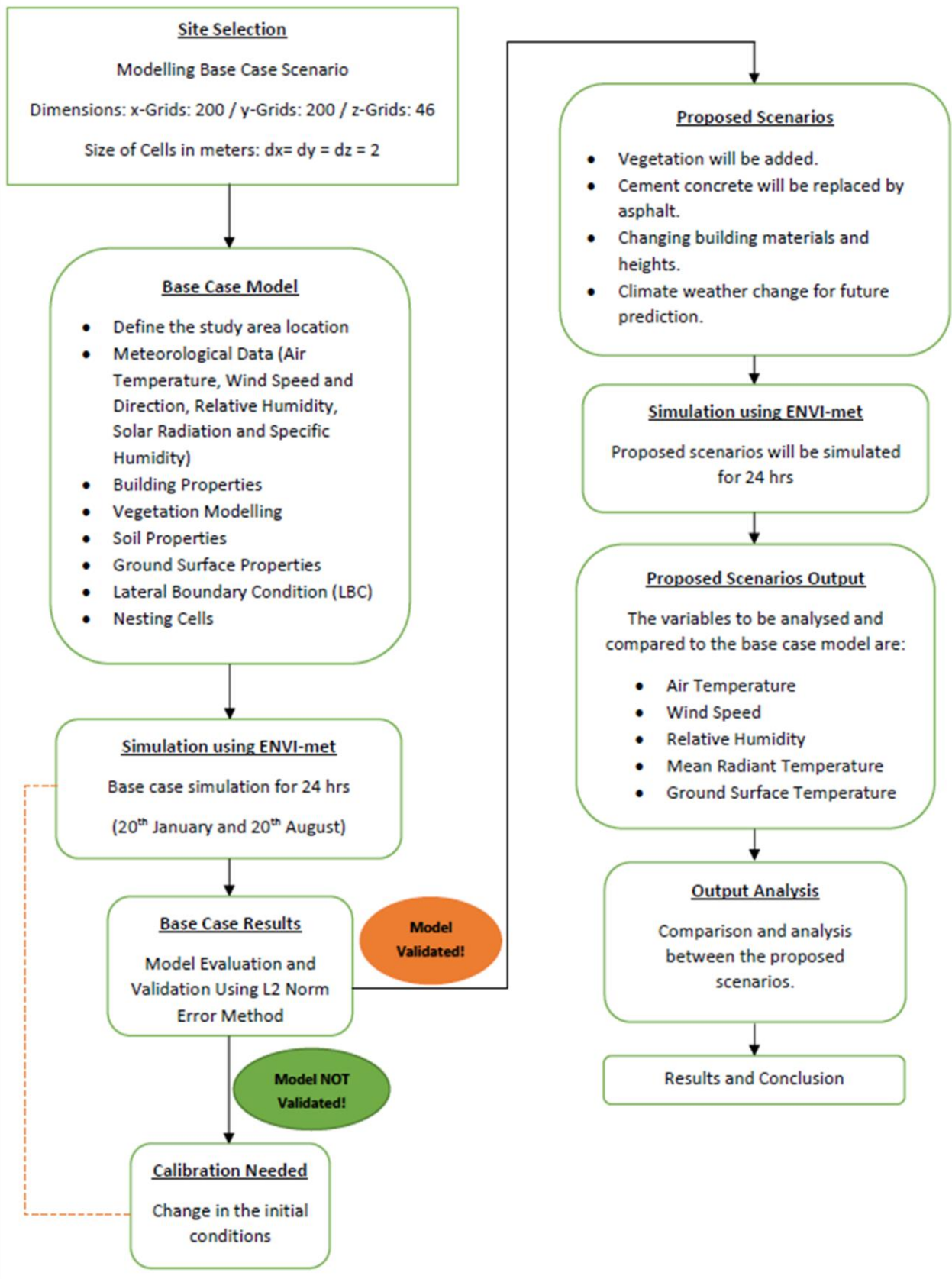


Figure 5. Flow Chart of the Study Methodology.

3.2 Control Variables

The three main control variables that were selected for this study are shown in Table 1. The first variable is the ground cover that has been selected due to the different types of covers that help in improving the thermal characteristics and reducing the temperature due to the increase in the albedo fraction. The second variable, the vegetation, has been selected due to its cooling effect that helps improve the thermal conditions in urban spaces such as air temperature, relative humidity and mean radiant temperature. The evaporative cooling process that occurs as a result of the conversion of sensible heat to latent heat facilitates the dissipation of the trapped heat in any urban geometry (Bowler, D.E., Buyung-Ali, L., Knight, T.M., Pullin, A.S., 2010). The third variable is replacing the old buildings with new ones. A survey was done in the studied area to define which of the building were old (age before 1995). The new buildings were constructed using masonry heavyweight concrete double wall with a 5mm air gap in between, in addition to double glazing windows. Building materials specifications effect the temperature when exposed to solar radiation, hence transferring heat to nearby environment.

Variables Assessment criteria	Ground Cover	Vegetation	Changing Old Buildings with New Ones.
Air Temperature	X	X	X
Wind Speed	X	X	X
Relative Humidity	X	X	X
Mean Radiant Temperature	X	X	X
Ground Surface Temperature	X	X	X

Table 1. Controlled variables with their assessment criteria.

3.3 Base Case Scenario

The base case scenario was simulated using ENVI-met V4.4. The advantage of ENVI-met is that it seeks to reproduce the processes in the atmosphere that affect the microclimate on a physical basis. This software has been used in many UHI studies (Tsilini, V., Papantoniou, S., Kolokotsa, D. D., & Maria, E. A. , 2015). This holistic microclimate model, couples thermodynamics and fluid dynamics in complex urban geometry and simulates the surface-plant-air interactions in an urban environment with a typical resolution down to 0.5 m in space and 1-5 sec in time (Bruse, M., 2016). The ENVI-met climate model will be used to simulate urban climate parameters, such as air temperature, relative humidity, wind velocity, and mean radiant temperature.

ENVI-met is a widely considered software that has been one of the most accurate models that can support in understanding the impact of the environment on the microclimate (Lee, H., Mayer, H., Chen, L., 2016) (Middel, A., Häb, K., Brazel, A.J., Martin, C.A., Guhathakurta, S., 2014). For example, a study compared three areas in Phoenix and found that the difference between the measured and modeled temperatures was minimal ($\Delta=0.4^{\circ}\text{C}$) (Middel, A., Häb, K., Brazel, A.J., Martin, C.A., Guhathakurta, S., 2014).

The layout of the chosen area was developed based on a satellite image obtained from Google Earth Pro software and field measurements. The completed area input file was 200 grids in the x and y directions, while 46 grids in the z-direction. Each grid cell in the area input file was set to be 2 by 2 meters in the x-y plane and 2 meters in the z-direction. In addition, a border of 15 nesting grids surrounded the simulation area for numerical stability. Regarding the tree species, the trees in the studied area were not found in the database of the ALBERO toolbox in ENVI-met, thus a study about the trees was done in order to build them in the software. The type of the trees, in addition to their height, total number of trees, and foliage albedo that controls the solar radiation incidence on the surface standing below it are

presented in Table 2. To create the tree in ALBERO, the following characteristics must be available: the height and the width of the plant, leaf density area (LAD), as well as the maximum depth of the roots and the root area density (RAD). Table 3 represents the thermal characteristics for both old and new building materials (Greenspec, 2018).

Type of Trees	Height of tree (m)	Foliage Albedo (α)	Quantity
Ficus Elastica	18	0.31	1
Ailanthus Altissima	18	0.28	1
Brachychiton Discolor	10	0.2	5
Syagrus Romanzoffiana	10	0.15	1
Eucalyptus Sp.	8	0.27	4
Ficus Retusa	7	0.27	1
Ligustrum Lucidum	7	0.2	1
Ficus Benjamina	6	0.28	1

Table 2. Type and total number of trees in the studied area.

	New Buildings	Old Buildings
Material Used	Masonry Heavyweight	Concrete Hollow Block
Thickness	0.25 m	0.20 m
Absorption	0.65	0.7
Transmission	0	0
Reflection	0.35	0.3
Emissivity	0.94	0.9
Specific Heat Capacity (J/Kg.K)	1000	840
Thermal Conductivity (W/m.K)	1.13	0.73
Density (Kg/m³)	2020	1500

Table 3. Thermal characteristics for building materials.

ENVI-met ran for a 24-hour simulation starting at 7:00 AM. The software will simulate hourly output for the temperature, wind speed, relative humidity, mean radiant temperature, and ground surface temperature, as well as many other variables and properties that are not used in this analysis.

3.3.1 Input Parameters

Tables 4 and 5 show the input parameters needed for the simulation as well as the road characteristics. Most of the surfaces were set to be the default soil type while the roads were created using the asphalt road.

	20 th January	20 th August
Starting time	7:00 AM (24 hrs.)	7:00 AM (24 hrs.)
Air Temperature	12°C	32°C
Wind Speed	2 m/sec	1.3 m/sec
Wind Direction	170 (South-East)	220 (South-West)
Relative Humidity	60 %	65 %
Lateral Boundary Condition	Cyclic	Cyclic
Building Interior Temperature	23°C	21°C

Table 4. Model configuration and initialization parameters for the simulations.

	Surface Albedo	Thickness (m)	Volumetric Heat Capacity (J/m ³ . K)
Asphalt Road	0.2	0.3	2.25
Cool Pavement	0.7	0.2	2.08

Table 5. Road characteristics for the simulations.

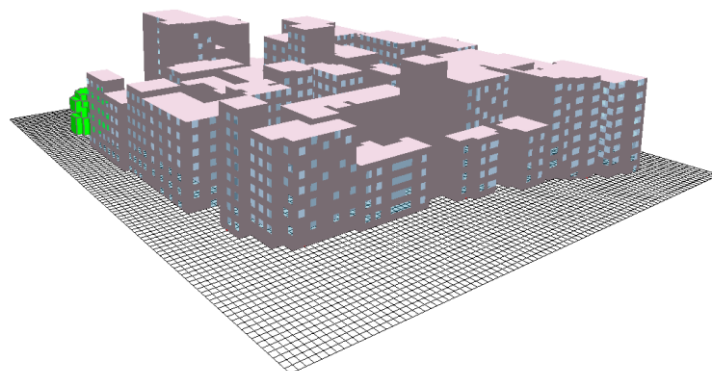


Figure 6. 3D Model Area by ENVI-met.



Figure 7. Pedestrian sidewalk illustrated on the base case scenario.

3.4 Proposed Scenarios

The proposed scenarios that were simulated in addition to the base case are shown in Table 6.

The first case scenario will replace the asphalt cover with cement concrete cover that has higher surface albedo. The fraction of albedo of the cool pavement is 0.7 (Table 5), whereas that of the asphalt road is 0.2. The second scenario (figure 9) will increase the cover of vegetation (type: Ficus Elastica) in the total area by 25%. Ficus Elastica is a broadleaf evergreen tree, which is planted across the sidewalks and pedestrian streets to provide enough shade and high foliage albedo. For the third scenario, old buildings, according to their age and height, were replaced with new high-rise developments as allowed by the local building law regulations figure 10, as mentioned before. In the fourth scenario, all the scenarios will be consolidated into one scenario to study the combined effect of all the parameters. A climate change scenario will be tested in addition to the following proposed scenarios for future prediction while keeping the controlled variables the same as the base case scenario and changing the initial air temperature value.

	Ground Cover	Vegetation Cover of the Total Area (%)	Building Heights and Materials
Base Case Scenario	Asphalt Cover	1 %	<ul style="list-style-type: none"> • Single & Double wall buildings • Single and Double glass windows
First Scenario	Cement Concrete Cover	1 %	<ul style="list-style-type: none"> • Single & Double wall buildings • Single and Double glass windows
Second Scenario	Asphalt Cover	26 %	<ul style="list-style-type: none"> • Single & Double wall buildings • Single and Double glass windows
Third Scenario	Asphalt Cover	1 %	<ul style="list-style-type: none"> • Double-wall buildings • Double glass windows
Fourth Scenario	Cement Concrete Cover	26 %	<ul style="list-style-type: none"> • Double-wall buildings • Double glass windows

Table 6. Proposed scenarios with their controlled variables.



Figure 8. First scenario, replacing asphalt cover with cool pavement. (*Heat Island, n.d.*)



Figure 9. Second scenario with 25% vegetation added to the base case.

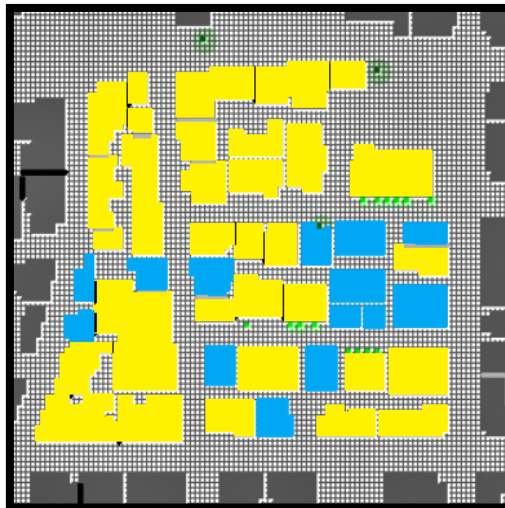


Figure 10. Third scenario where blue colored old buildings were replaced with new ones.

3.5 Outdoor Thermal Comfort

Adding urban vegetation strategy (second scenario) was chosen for studying its effect in outdoor spaces and on enhancing the outdoor thermal comfort. Two streets (S1 and S2) were chosen in the studied area with different orientations (figure 11).

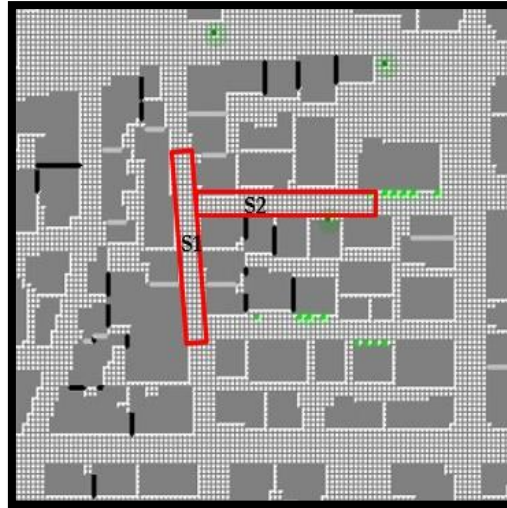


Figure 11. Base case scenario with S1 and S2 streets

Thermal comfort is referred to as an indicator to describe people's individual experiences of temperature in urban open spaces. It is also defined as ‘the condition of mind which expresses satisfaction with the thermal environment’ (ASHRAE, 2009). The assessment of the thermal comfort was based on PET (physiological equivalent temperature).

To calculate the PET, information about the personal human parameters (Table 7) should be provided in addition to the clothing parameters. These are needed for the energy balance of the body, which enables assessment of the comfort in a surrounding environment. The total metabolic rate is known as the internal energy production by the body. However, the clothing insulation is the thermal resistance of the clothing and mainly 0.5 clo for summer clothes and 1.5 for winter clothes (ASHRAE, 2009). PET expands the human thermal comfort to a standard index with units of $^{\circ}\text{C}$, as shown in Table 8.

	Input
Weight (Kg)	70
Height (m)	1.75
Surface Area (m²)	1.9
Walking Speed (m/s)	1.2
Clothing Insulation (clo)	0.5
Total Metabolic Rate (W)	166.46

Table 7. Setting for PET Calculation.

Grade of Physiological Stress	Thermal Perception	PET °C	PMV
Extreme Cold Stress	Very Cold	< 4	< -3.5
Strong Cold Stress	Cold	4 - 8	-3.5 - -2.5
Moderate Cold Stress	Cool	8 - 13	-2.5 - -1.5
Slight Cold Stress	Slightly Cool	13 - 18	-1.5 - -0.5
No Thermal Stress	Comfortable	18 - 23	-0.5 - 0.5
Slight Heat Stress	Slightly Warm	23 - 29	0.5 - 1.5
Moderate Heat Stress	Warm	29 - 35	1.5 - 2.5
Strong Heat Stress	Hot	35 - 41	2.5 - 3.5
Extreme Heat Stress	Very Hot	> 41	> 3.5

Table 8. Thermal sensation according to PMV and PET values.

3.6 Climate Change and Future Prediction

Mitigation strategies should be considered to reduce the impact of climate change in the future. To study the impact of the climate change in Beirut City and to predict what will be the case in the future if no action will be taken by the municipality of Beirut and without implementing the mitigation strategies, the base case study will be repeated for the summer season by only increasing the air temperature of the initial parameters from 32°C to 37°C (Pachauri, R. K., Allen, M. R., Barros, V. R., Broome, J., Cramer, W., Christ, R., ... & Dubash, N. K. , 2014). Regarding wind speed, several studies predicted that the changes in the annual mean would be less than +/- 0.2 m/s while other individual models predicted wind

speed differences of +/- 0.5 m/s (Eichelberger et. al, 2008). In this study, the initial wind speed was assumed constant as the base case scenario.

CHAPTER 4

LATERAL BOUNDARY CONDITIONS AND NESTING CELLS

In this chapter, the three types of lateral boundary conditions (LBC) used in ENVI-met will be described, in addition to boundary condition chosen for our study. The second part of the chapter will be related to the nesting cells and the number of nesting cells chosen before starting the simulation.

4.1 Lateral Boundary Condition

Lateral boundary conditions (LBC) were defined in three different types that allow ENVI-met to manage the boundaries of the model for turbulence (Bruse, M., 2016):

- “Closed (or Forced) Boundary Conditions”: the values of the one-dimensional model are copied to the border,
- “Open Boundary Conditions”: the values of the inner points are copied back to the lateral inflow boundary for each time step,
- “Cyclic Boundary Conditions”: the values of the downstream model border are copied to the upstream model border.

The open and cyclic lateral boundary conditions differ from the forced boundary condition by allowing the simulation to start with few initial parameters. Closed boundary conditions allow the air temperature and the relative humidity to be forced through the diurnal cycle along with the simulation. The forced LBC is the most stable condition as it uses the 1-D model to obtain the boundary values, which stabilizes the 3-D model. The open LBC is the condition when the values are copied from the inner parts of the model to the boundaries with the minimum effect of the model boundary onto the inner parts of the model. Finally, the cyclic LBC is the condition that assumes that the average conditions of the upstream conditions are similar to the model area (Bruse, M., 2016; Simon, H., 2016). In other words,

choosing the appropriate lateral boundary condition is solely dependent on the concerned model.

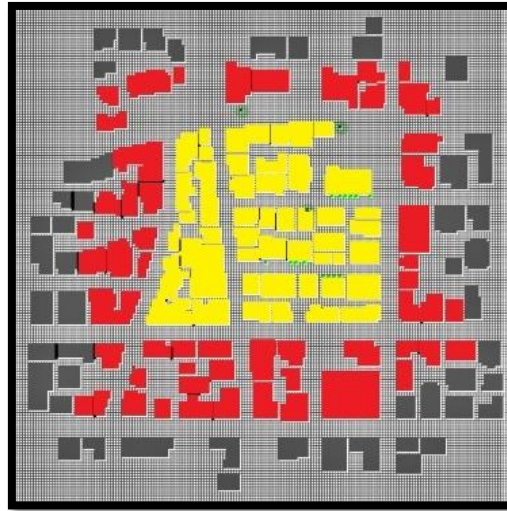


Figure 12. Input file drawing for ENVI-met simulations.

Figure 12 represents the input file drawing for ENVI-met simulation. The yellow colored buildings represent the interest area being studied. The red colored buildings were added on the periphery of the studied area for numerical stability and represent the base case area. No meteorological data were measured on site due to lack of weather station in the studied area. Therefore, an outer ring of buildings which is represented by the grey color will play the role as a reference case that will make the studied area fully stable and will be compared to each other using the L2 norm method. A study showed that high resolution is required to include all the geometric details but is also necessary to add part of the surroundings to get contentment results for the area of interest (Chatzidimitriou, A., & Axarli, K. , 2017). Both forced and cyclic LBC were studied to check which LBC best suits the studied area and to be adopted. First, only the studied area was simulated for both boundary conditions. For the forced LBC, the meteorological data was added hourly from the weather underground website due to the lack of weather stations in the studied area. On the other hand, the cyclic

LBC needed only initial input at the beginning of the simulation. Comparing the results, there was a difference between the two LBC even though the same number of nesting cells were used. As a result, the periphery area of buildings was added to check the effect of adding an extra layer of building on the results of the studied area. The results show that both LBC leads to a minimal difference in the air temperature and no difference in the wind speed results.

These results presented the importance of increasing the area of building outside on the border of the studied area, which lead to numerical stability and how the results would differ if only the studied area was simulated alone. Therefore, the cyclic lateral boundary condition was adopted since it represents a model where the neighborhood has, on average, the same structure as the model area and being very close.

4.2 Nesting Cells

The nesting cells are grids that surround the simulated area to maintain the numerical stability and to reduce the effects of the chosen boundary. In the computational domain, nesting grids was added for creating a zone in both x and y directions, thus generating a way that will reduce the numerical instability by moving the model boundary away from the studied area.

To study the importance of adding a periphery building layer around the studied area and the effect of the nesting cells, several case studies were tested for that purpose. Table 9 shows that two reference cases A and B were selected, which is the base case with an extra periphery layer of buildings, as shown in figure 12, with a different number of nesting cells. Cases 1 and 2 were only the studied area without the addition of any periphery buildings with nesting cells equal 15 and 5, respectively. While for cases 3 to 5, which is the base case, it was the studied area in addition to the periphery buildings.

Cases 1 to 5 will be compared for both reference cases, and the assessment parameters will be the air temperature and the wind speed.

Cases	Model Area Type	Nesting Cells
Reference Case A	Base Case with an extra periphery layer of buildings	15
Reference Case B	Base Case with an extra periphery layer of buildings	5
Case 1	No Periphery Buildings were added	15
Case 2	No Periphery Buildings were added	5
Case 3	Base Case with Periphery Buildings	15
Case 4	Base Case with Periphery Buildings	5
Case 5	Base Case with Periphery Buildings	1

Table 9. Different model areas with different numbers of nesting cells.

CHAPTER 5

Results

The following section presents the results relating to the nesting cells, the base case simulation as well the scenarios that were conducted. I would also like to add that the base case scenario is referred to as BCS, cool pavement scenario as CPS, new buildings scenario as NBS, vegetation scenario as VS, and the combined case scenario as CCS.

4.1 Model Validation using L2 Norm Method

The five cases were compared using the L2 norm error with reference cases A and B. The focus during the calculation of the error will be the studied area. For both air temperature and wind speed, cases 1 and 2 showed the maximum error percentage among the five cases. On the other hand, cases 3 to 5 showed less error percentage compared to cases 1 and 2.

Comparing the five cases, case 3 that includes the periphery buildings outside the studied area, showed the minimal error compared to the reference case B which has 0.26% error for the air temperature and 0.75% error for the wind speed.

Also comparing case 1 and case 3 that have the same number of nesting cells, and after adding the periphery building layers for case 3, the error decreased for the air temperature from 7.48% to 0.69% and the wind speed from 41.58% to 1.06% with respect to reference case A. Comparing cases 3 to 5, that have the same model area type but a different number of nesting cells, showed that case 3 has the least error percentage with respect to the reference cases.

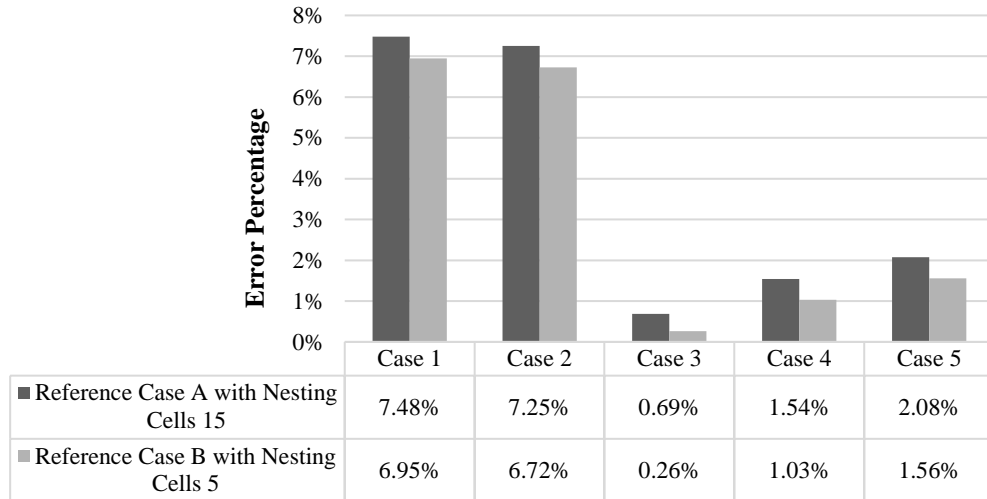


Figure 13. Air temperature comparison between Reference and other cases using L2 norm error method.

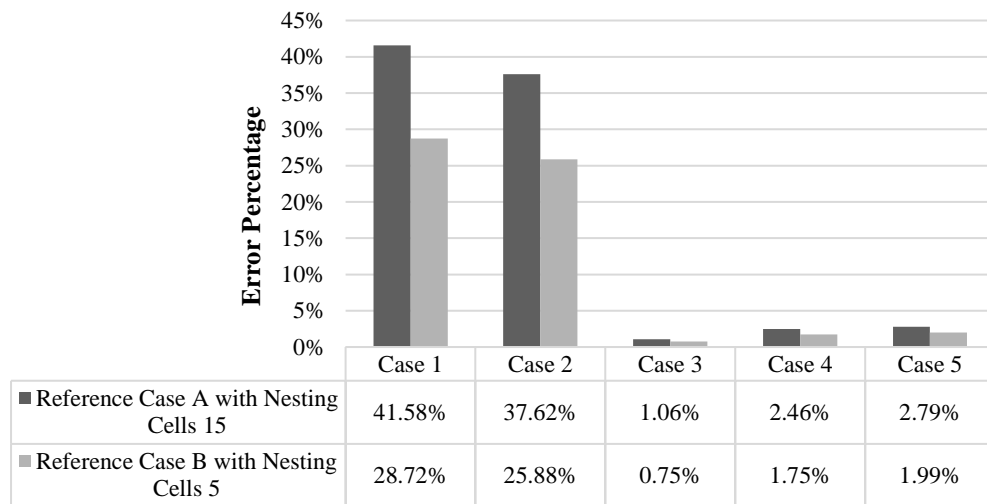


Figure 14. Wind speed comparison between Reference and other cases using L2 norm error method.

This comparison revealed the importance of increasing the periphery buildings around any studied area thus reaching numerical stability, and how the results will be affected if only the base case were simulated without adding the layer of buildings. Also, the comparison showed that the nesting cells are responsible for maintaining numerical stability, but it didn't have the same effect as the boundary layer of buildings.

The following results show the comparison between the base case and other mitigation scenarios at 1.4m height for air temperature (T_a), wind speed, relative humidity, and mean radiant temperature (T_{mrt}), while the ground surface temperature (T_s) results will be at the ground level, on summer and a winter day.

4.2 Air Temperature

Figure 15 showed that all the cases had lower T_a except for the climate change, which revealed higher T_a , while no difference between the BCS and the NBS. The maximum decrease in the T_a was at 17:00 between the BCS and the CCS, which is 2.6°C , while the increase in the T_a for the climate change was maximum during the night-time reaching 1.8°C .

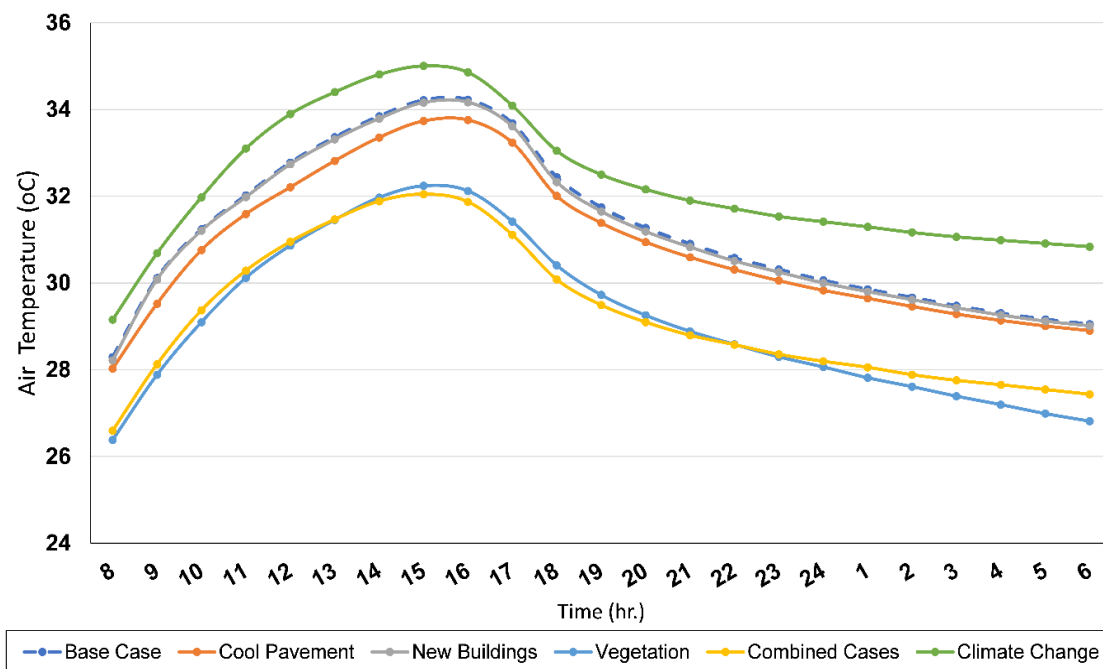


Figure 15. Comparison of hourly average air temperature results for different scenarios on August 20th.

Figure 16 which refers for a winter day, showed that there is no difference in T_a between the BCS and the CPS, while the VS and the CCS showed the same results with a difference 0.9°C compared to the BCS during the day time, and a decrease to 0.5°C during the night time.

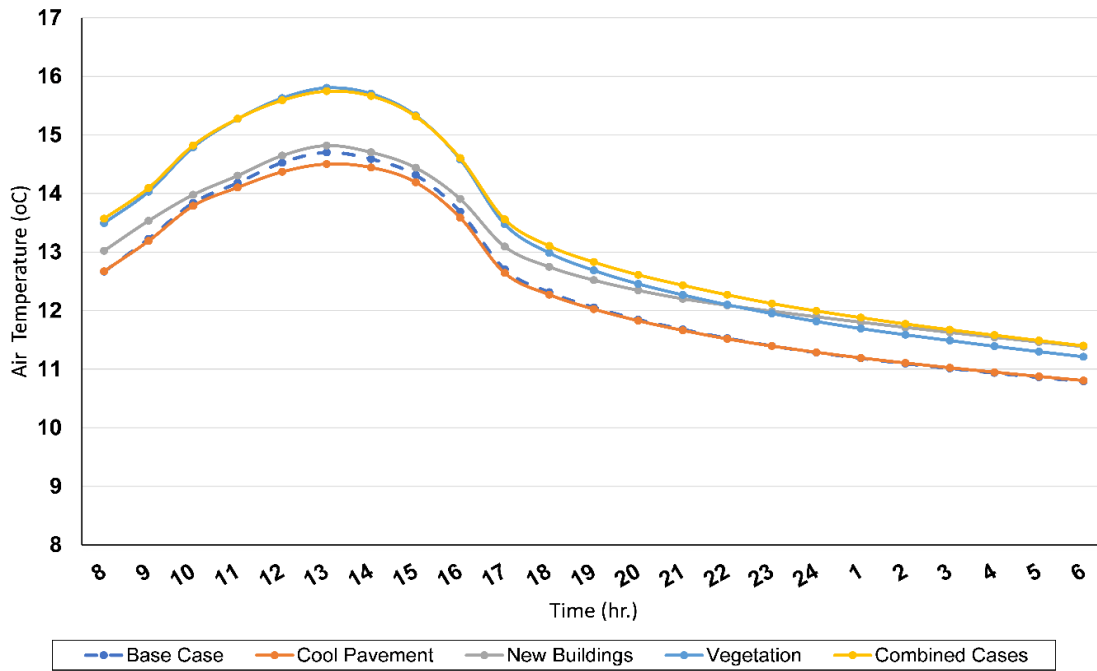


Figure 16. Comparison of hourly average air temperature results for different scenarios on January 20th.

Figure 17 shows the absolute difference in the air temperature between the BCS and various heat mitigation strategies at 12 noon in addition to the solar orientation and wind direction. There is a slight difference in Fig.17 (a) compared to the BCS, while the maximum difference is for the two scenarios, the VS and the CCS, Fig.17 (c, d). For the climate change scenario, Fig.17 (e), the absolute difference for the T_a is different from the other scenarios because the climate change scenario shows a higher temperature than that of the BCS, same as in figure 15.

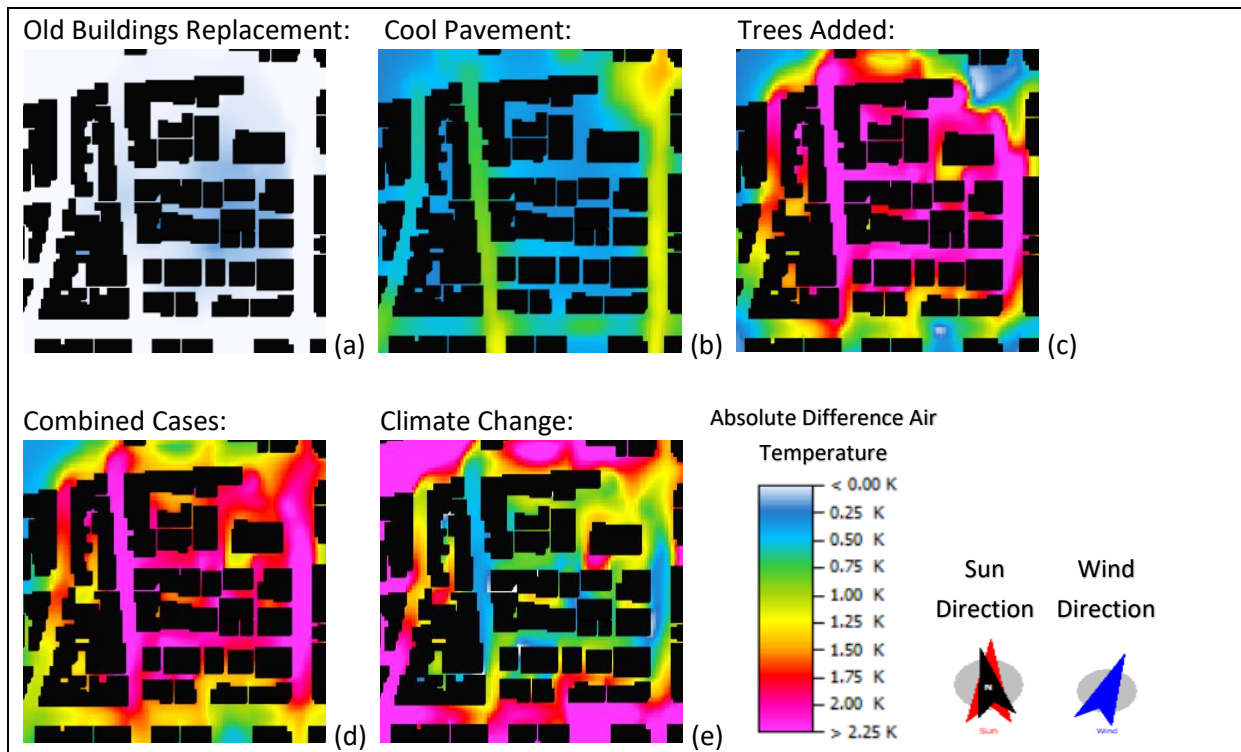


Figure 17. Absolute difference in air temperature between various heat mitigation scenarios and the base case scenario at 12:00 at 1.4m elevation from ground level.

4.3 Wind Speed

ENVI-met simulation in Figure 18 shows the average wind speed difference among the cases in addition to the BCS on a summer day (August 20th). The mean wind speed at the pedestrian path sidewalk for all cases shows higher wind speed except for the scenario of the NBS. There is a very slight difference between the BCS and the CPS, while the maximum difference is between the BCS and the climate change scenario, which is 0.08 m/sec.

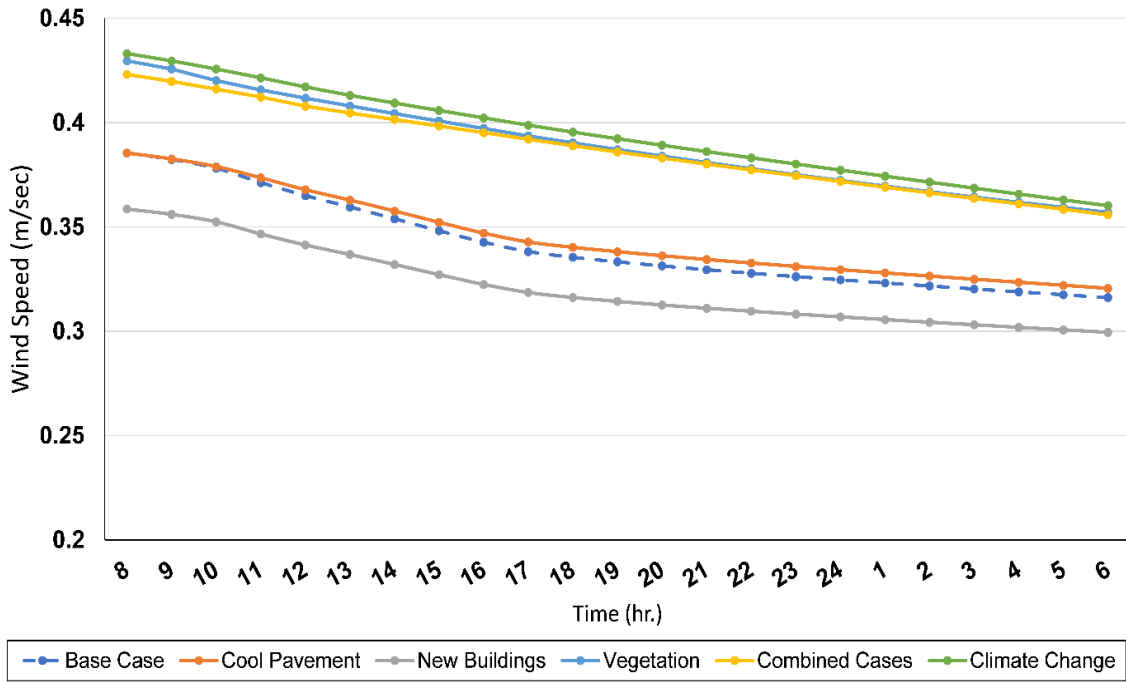


Figure 18. Comparison of hourly average wind speed results for different scenarios on August 20th.

Figure 19 that refers to a winter day (20th January) shows no difference between the base case, cool pavement, and new buildings, while 0.15 m/sec difference between the base case and the vegetation and combined case scenarios.

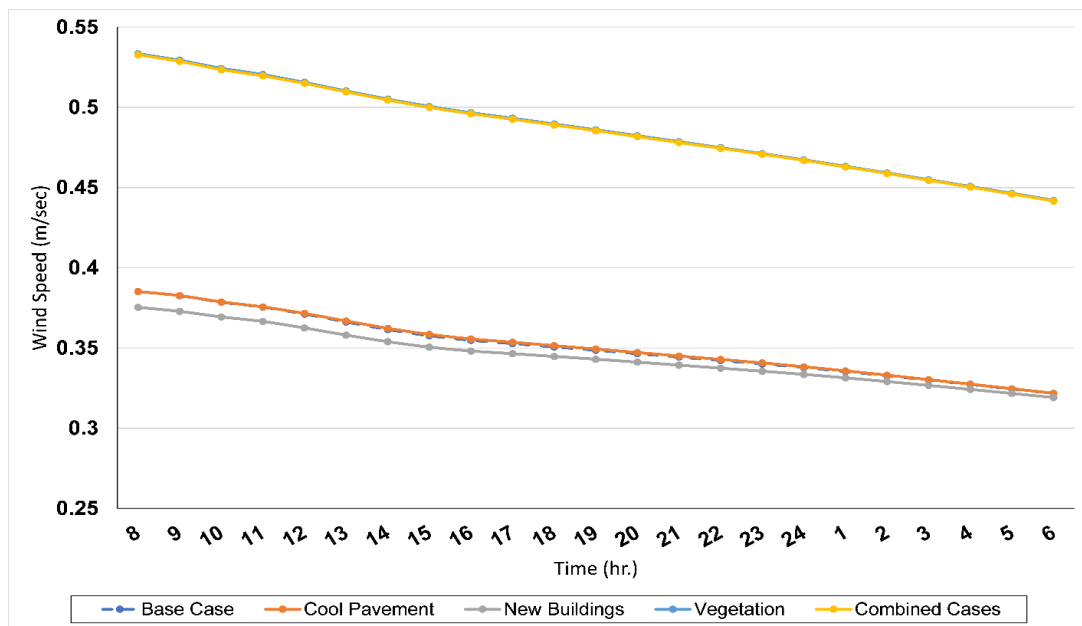


Figure 19. Comparison of hourly average wind speed results for different scenarios on January 20th.

Figure 20 shows the absolute difference in the wind speed between the proposed scenarios and the base case scenario at 12 noon. Fig.20 (c,d,e) shows the difference between the scenarios and the BCS, while Fig.20 (a) shows a small difference between the NBS and the BCS. As for the CPS Fig.20 (b), there is no difference compared to the BCS.

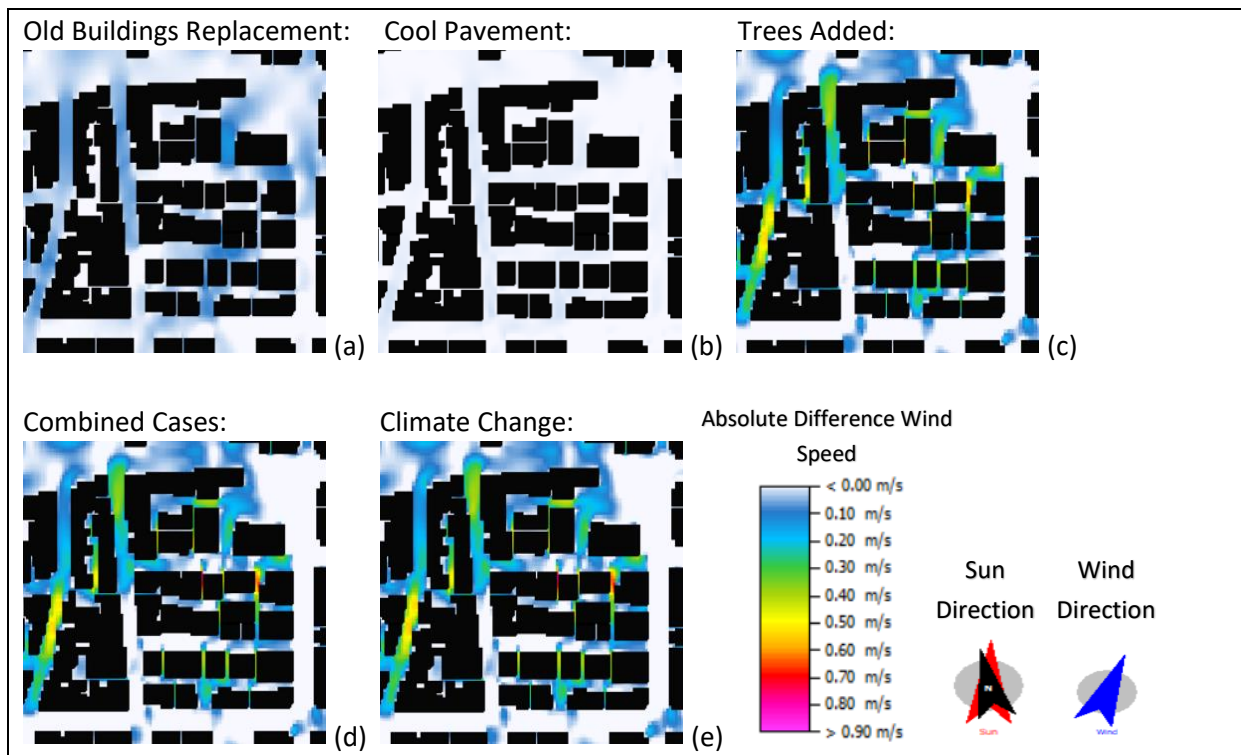


Figure 20. Absolute difference in wind speed between various heat mitigation scenarios and the base case scenario at 12:00 at 1.4m elevation from ground level.

4.4 Relative Humidity

Figure 21 which refers to relative humidity at 1.4 m height for a summer day, shows that all the cases have higher relative humidity compared to the BCS, while no difference is between the BCS and the NBS. The maximum difference is between the BCS and the CCS, which reaches 18% during the daytime and decreases to 11% during the night-time hours. As for the climate change scenario, the maximum difference with respect to the BCS is during noon (24%), while decreasing to 15% during the night.

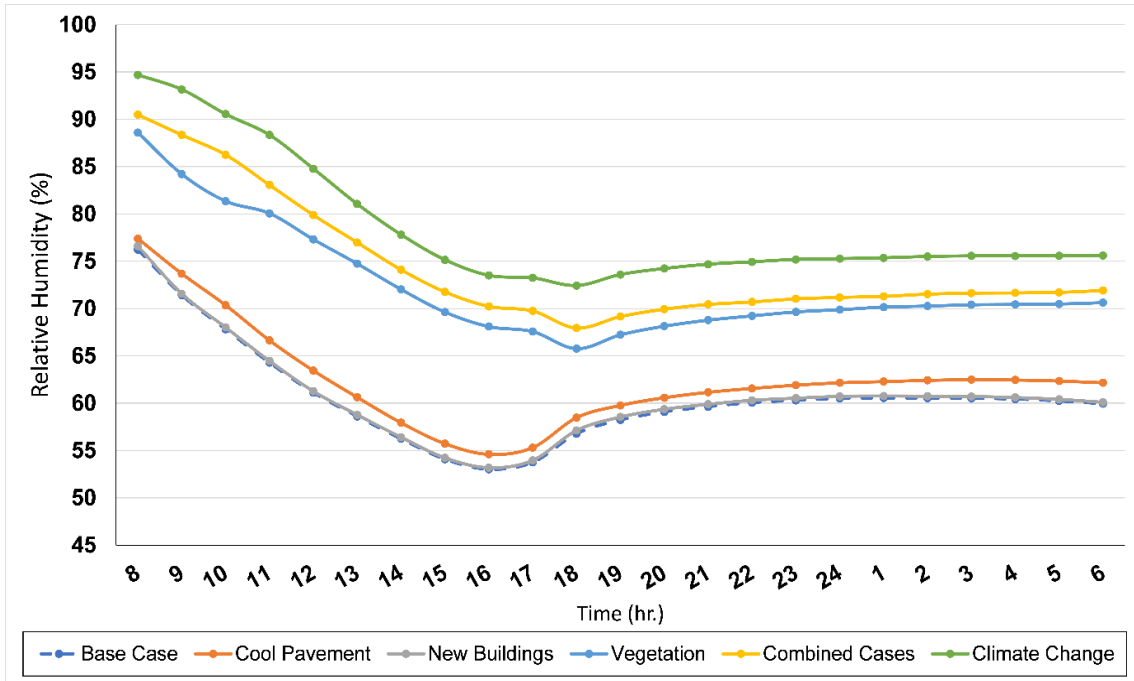


Figure 21. Comparison of hourly average relative humidity results for different scenarios on August 20th.

As for figure 22, which refers to a winter day, the relative humidity is increasing during the night hours. During the daytime, the relative humidity increased by 4.7% between the BCS and the CCS, while decreased during the night hours by 3%.

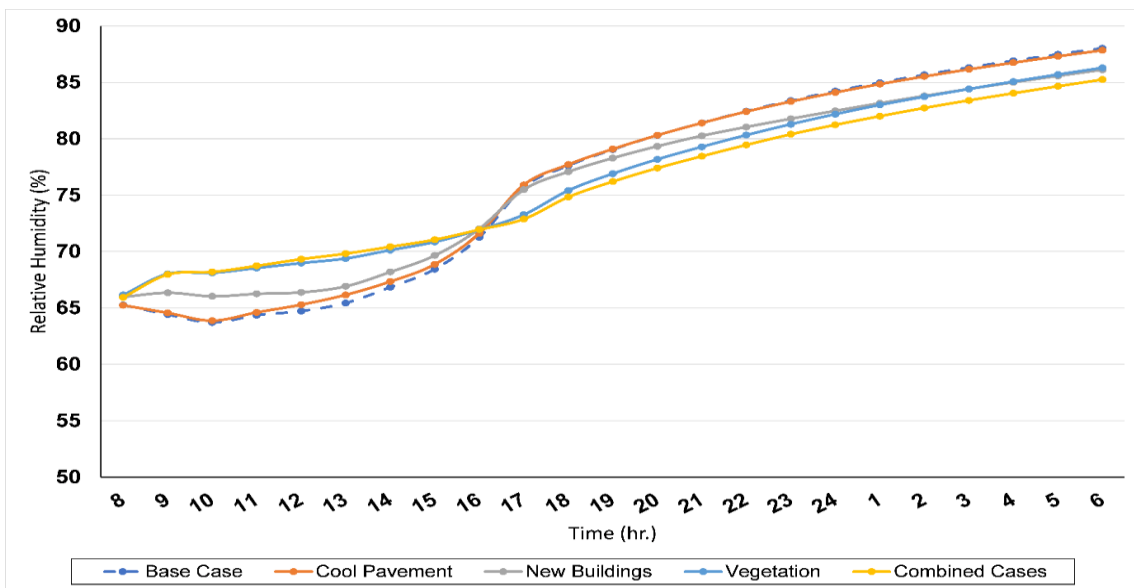


Figure 22. Comparison of hourly average relative humidity results for different scenarios on January 20th.

Figure 23 shows the absolute difference in the relative humidity between the BCS and various heat mitigation strategies at 12 noon. Fig.23 (a) shows that there is no effect of changing the NBS on the relative humidity. Adding cool pavement fig.23 (b) shows a slight increase in the relative humidity compared to the BCS. The maximum absolute difference for relative humidity is for the climate change scenario fig.23 (e) compared to the BCS reaching some areas to 27%.

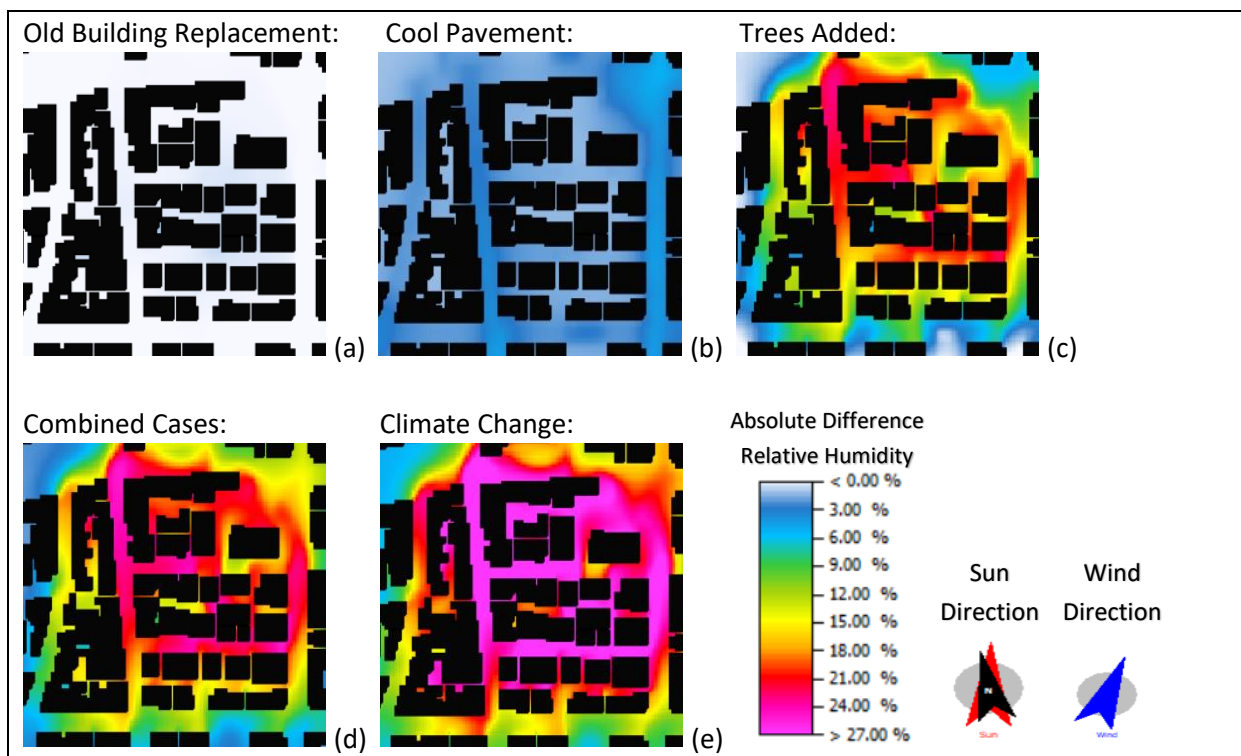


Figure 23. Absolute difference in relative humidity between various heat mitigation scenarios and the base case scenario at 12:00 at 1.4m elevation from ground level.

4.5 Mean Radiant Temperature

Figure 24 shows that during a summer day, all the cases have lower mean radiant temperature except for the CPS. The VS shows that the maximum difference reaches 10.5°C at noon, which is higher than the CCS due to the cool pavement. During the night, all the scenarios show no difference except for the climate change scenario, which increased by 4°C.

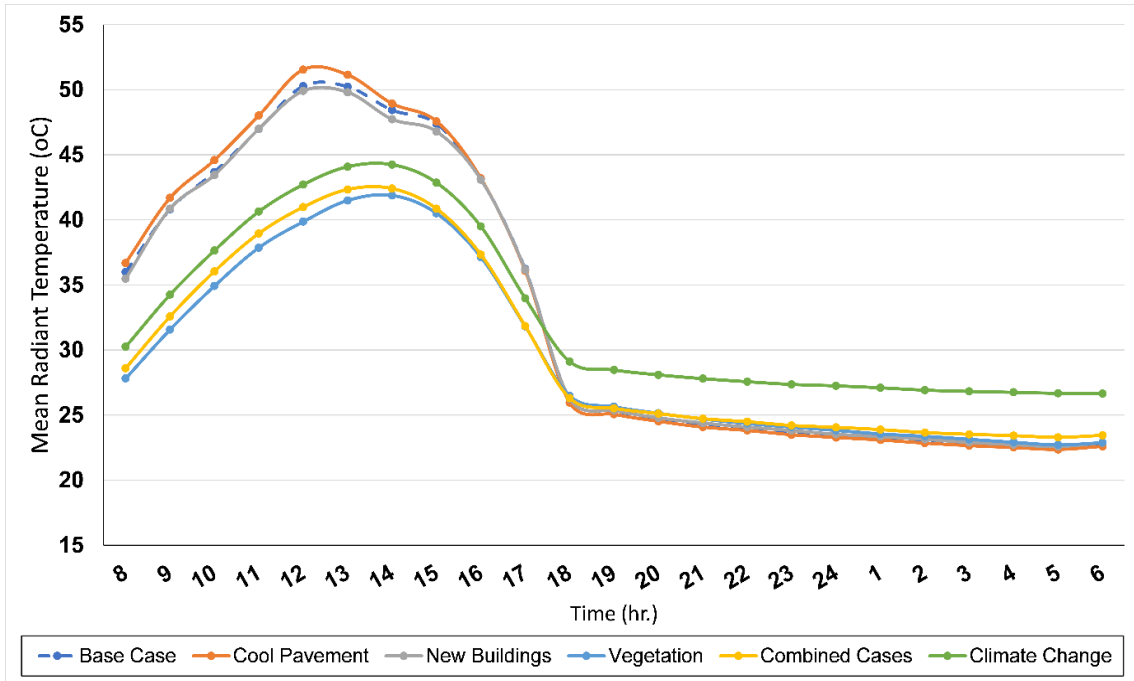


Figure 24. Comparison of hourly average mean radiant temperature results for different scenarios on August 20th.

As for figure 25, it shows that the maximum difference between the scenarios is at noon while a slightly difference during the night. The maximum difference at noon is between the BCS and the VS reaching 6.5°C, while a small difference between the BCS and the CPS and no difference compared to the NBS.

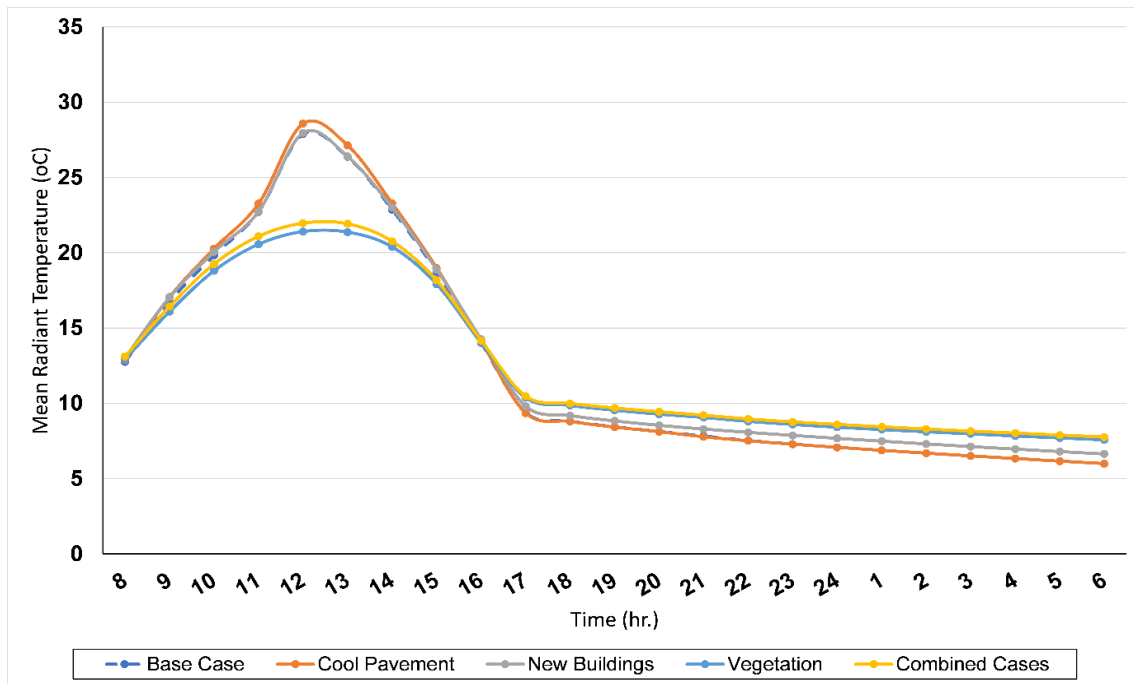


Figure 25. Comparison of hourly average mean radiant temperature results for different scenarios on January 20th.

Figure 26 shows the absolute difference in the mean radiant temperature (T_{mrt}) between the proposed scenarios and the BCS at 12 noon. Showing that the sun's location is due south direction, the NBS fig.26 (a) indicates some places near the buildings with a small difference compared to the base case. The maximum difference, which is the VS fig.26 (c), reaches almost 20°C, which is higher between the all other proposed cases. For the CPS fig.26 (b), it shows a higher mean radiant (2°C) compared to the base case scenario.

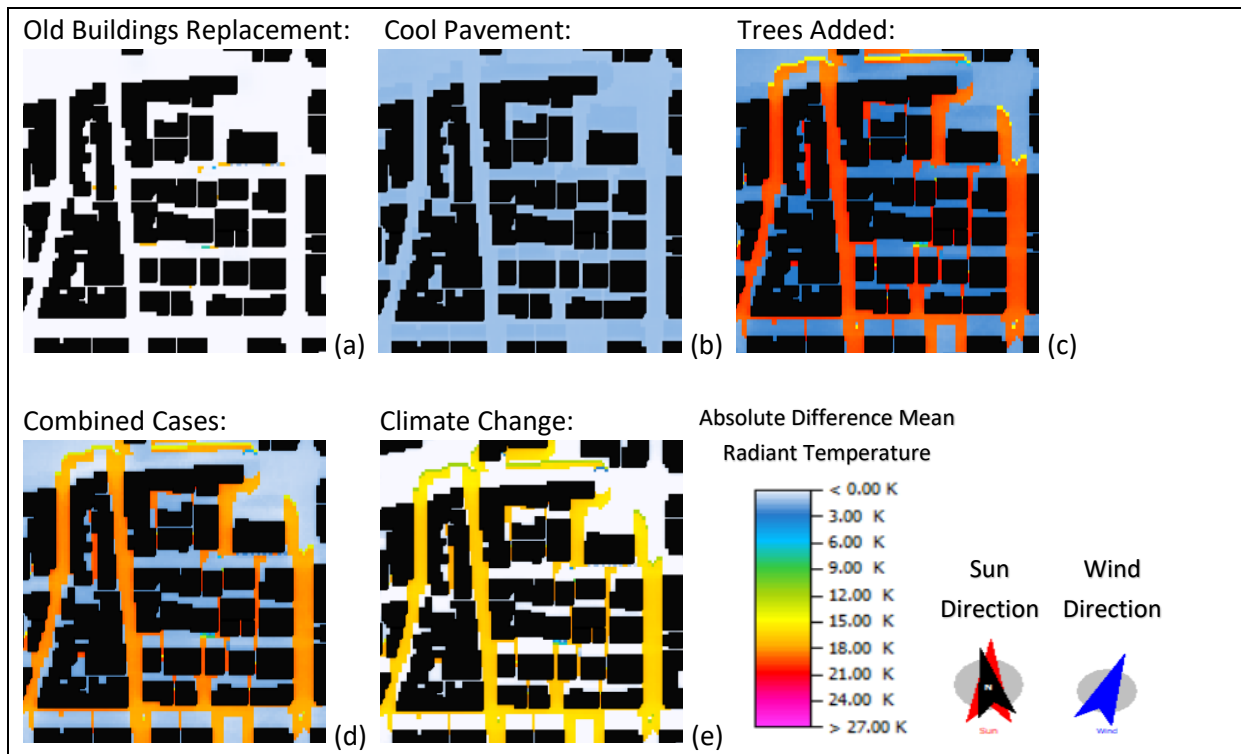


Figure 26. Absolute difference in mean radiant temperature between various heat mitigation scenarios and the base case scenario at 12:00 at 1.4m elevation from ground level.

4.6 Ground Surface Temperature

Figure 27 shows during the day that all the cases have lower ground surface temperature while no effect for the NBS. The only exception is for the climate change scenario during the night that shows higher ground surface temperature reaching 2.5°C compared to BCS. The maximum decrease in the ground surface temperature is at noon between the BCS and the CCS, which is 6.5°C.

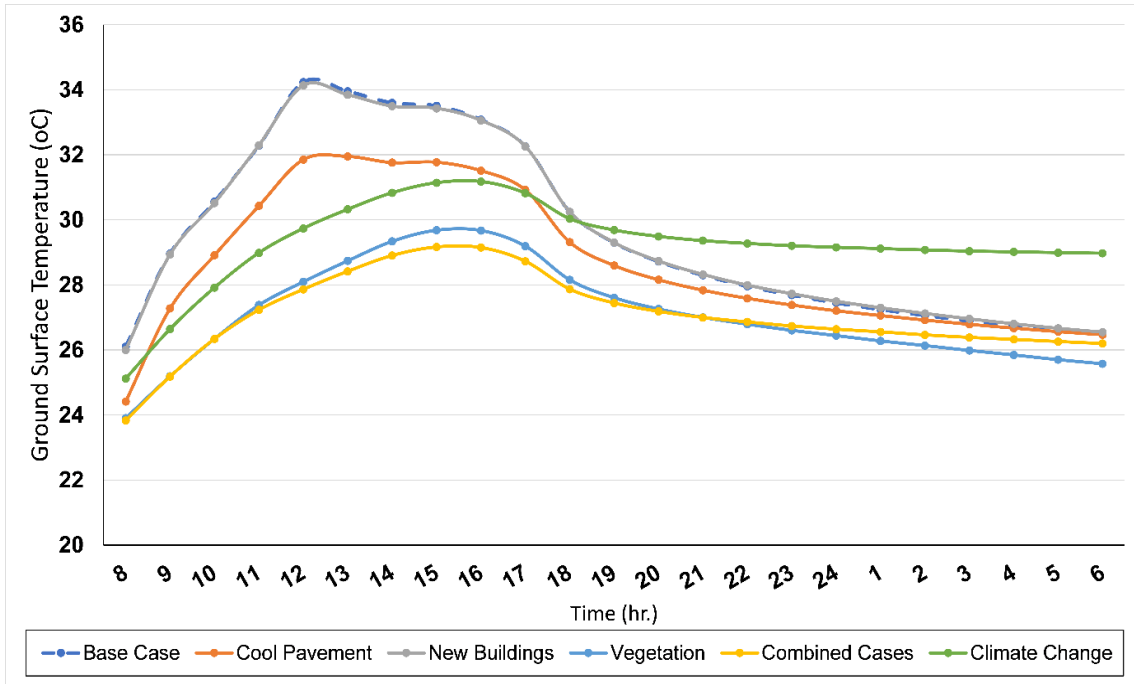


Figure 27. Comparison of hourly average ground surface temperature results for different scenarios on August 20th.

Figure 28 shows a small difference between the whole scenarios when compared to the BCS. The maximum difference at noon compared to the CCS reaching 0.8°C.

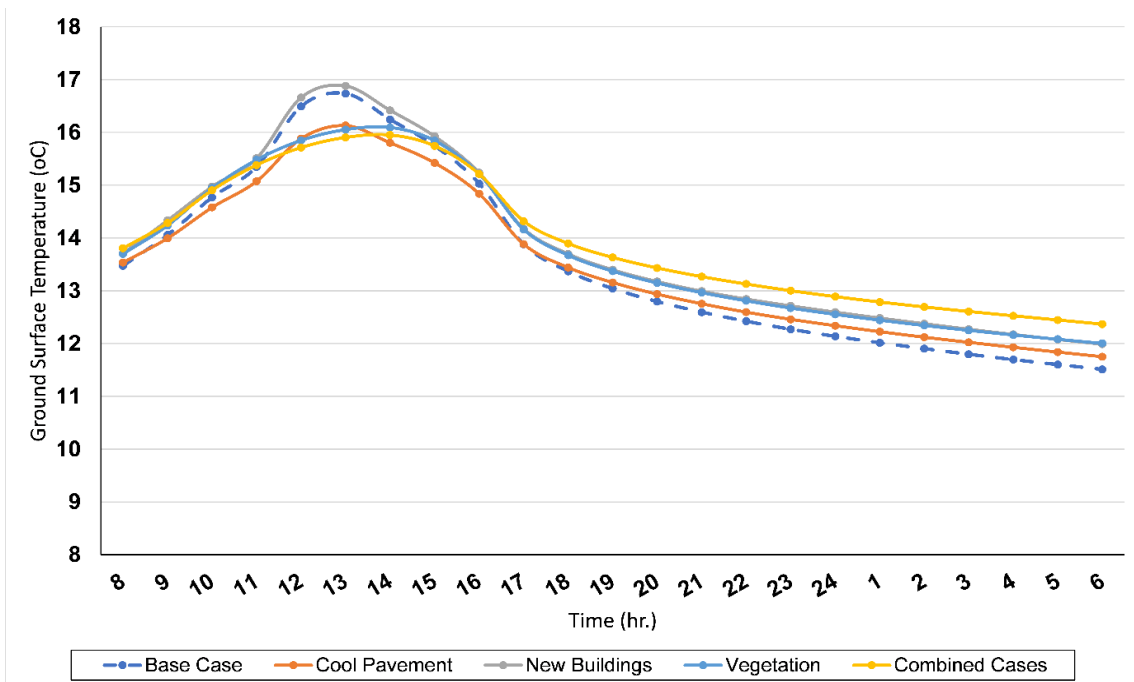


Figure 28. Comparison of hourly average ground surface temperature results for different scenarios on January 20th.

Figure 29 shows the absolute difference in the ground surface temperature (T_g) between the proposed scenarios and the BCS at 12 noon. The smallest effect among the proposed scenarios is the NBS fig.29 (a). Due to the sun's direction, the maximum difference is available on North-South streets. The maximum difference is compared to the CCS fig.29 (d) reaching in some areas 25°C and above, while the absolute difference compared to the climate change fig.29 (e) shows lower values than the combined cases (21°C).

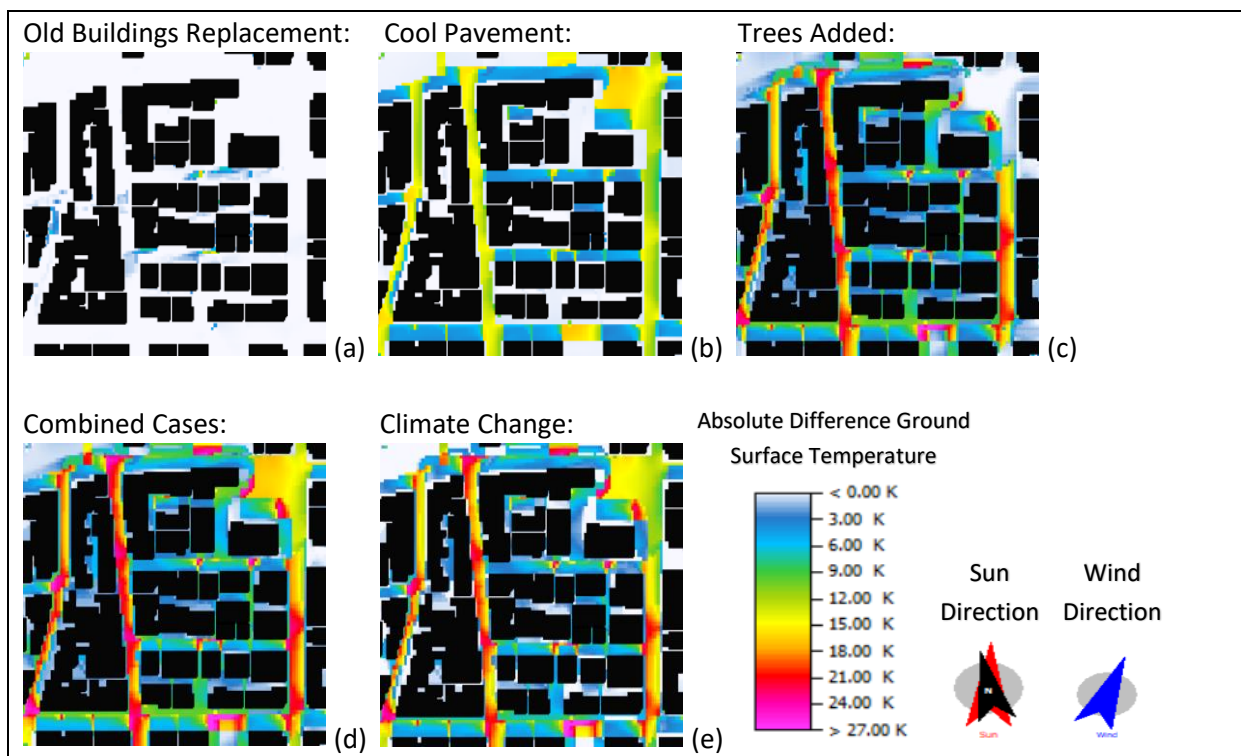


Figure 29. Absolute difference in ground surface temperature between various heat mitigation scenarios and the base case scenario at 12:00 at the ground level.

4.7 Outdoor Thermal Comfort

Figure 30 shows the thermal comfort change on a summer day (20th August) at the two streets at human height level 1.4 m. Adding the vegetation results in lower values of PET compared to the base case scenario at the two chosen streets. For street S1, the most significant reduction (12.6°C) was observed at 12:00 pm. The average PET reduction on the same street was found to be 2.81°C . However, for street S2, the most significant decrease after adding

the trees was observed at 9:00 am by 21°C due to the solar orientation, and the average PET reduction was found to be 3.8°C.

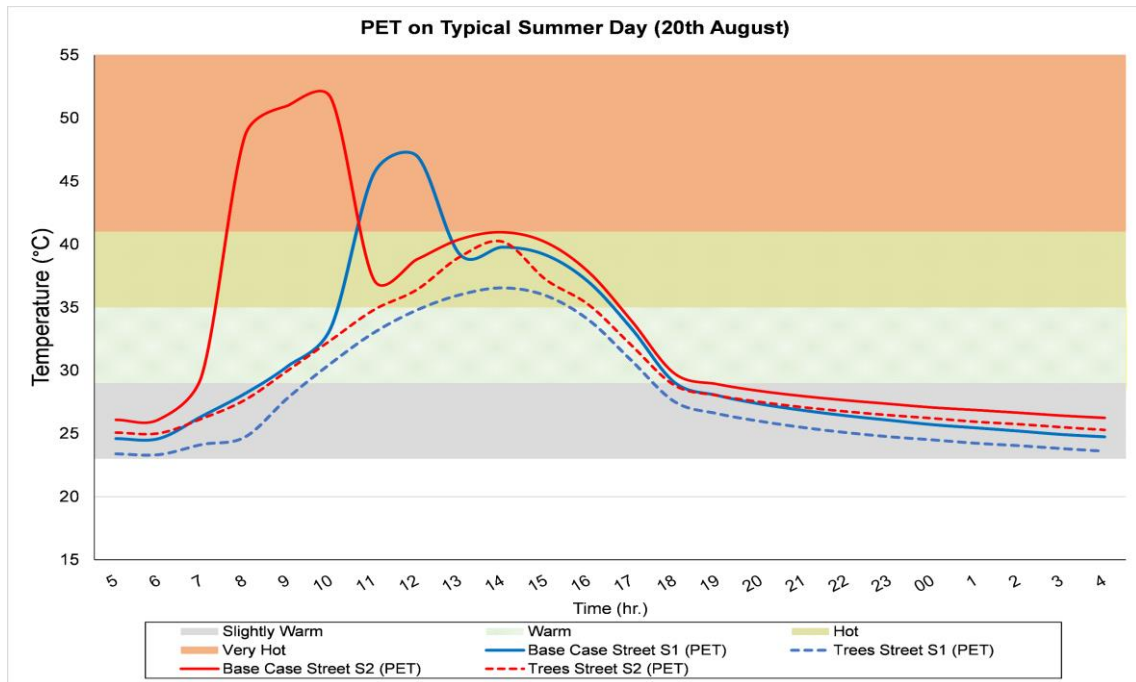


Figure 30. PET change at 1.4m above the ground level on a typical summer day (20th August) at two locations with the base case scenario and the vegetation scenario.

Figure 31 show the PET distribution map on a summer day at three different hours 8:00 am, 12:00 pm, and 16:00, respectively. The addition of trees and depending on the sun’s location results in lowering PET indices.

Besides, adding trees show that the vegetation scenario, has lower PET index (more comfortable) than the current base case scenario. Also, showing the figures of streets S1 and S2 with different PET values, give an idea about which street to be pedestrianized during the daytime.

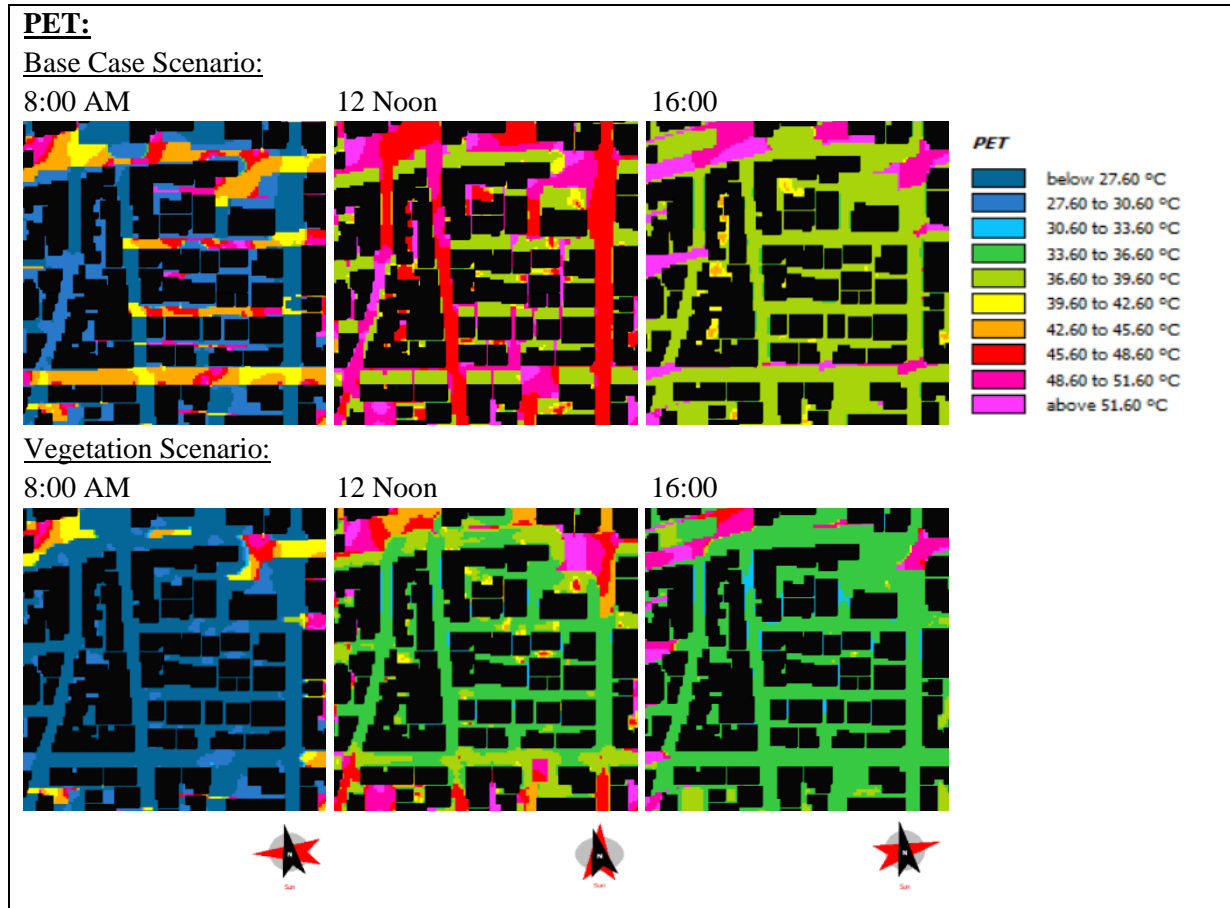


Figure 31. PET simulation for both scenarios at three different hours.

CHAPTER 6

DISCUSSION

According to the results presented in the previous section, August 20th is analyzed since it adequately show what the optimal mitigation strategy is for Beirut. The inclusion of vegetation induced the shade produced and evapotranspiration which lead to the decrease in air temperature and the cooling effect to happen.

Although several studies showed that the wind speed in the vegetated scenario is lower than the BCS, this study revealed that the wind speed after adding vegetation increased by 0.07 m/s. This was deduced from the results which only showed the mean wind speed at the pedestrian sidewalk pathway as opposed to being at a specific location. The relative humidity has an inverse relationship with the air temperature (Aboelata, A., & Sodoudi, S., 2019); thus, the vegetation scenario has the highest relative humidity values. Adding vegetation in the proposed scenario will lead to shaded space, thus a decrease in SVF, which is better than the thermal environment in an open space with high value in SVF. Therefore, increasing the urban vegetation in any area will protect the pedestrian from direct sunshine due to the shading produced, resulting in decreasing the mean radiant temperature and air temperature and improving the thermal comfort in the summer days (Jaafar, H., Lakkis, I., Yeretjian, A., 2020).

The CPS indicated higher mean radiant temperature than the BCS due to the increase in the albedo fraction of the ground cover because of the increase in the reflected radiation during the day. The decrease in the ground surface temperature is also in line with other studies where increasing the albedo by 0.25 leads to decrease in the surface temperature by 10°C (Akbari, H., Pomerantz, M., Taha, H., 2001). Other studies stated that the increase in the reflected solar radiation by reflective surfaces exceed the reduction in longwave radiation,

thus affect the thermal comfort of the pedestrian in a negative way. Therefore, the analysis revealed that the inclusion of vegetation in urban areas will significantly influence mitigating the UHI effects. In other words, it is the optimal mitigation strategy in comparison with the other strategies.

In addition, when studying the climate change to anticipate weather forecasts, an increase in air temperature resulted in the relative humidity and air temperature to increase throughout the whole day. Whilst the mean radiant temperature and ground surface temperature demonstrated higher values during the night.

CHAPTER 7

CONCLUSION

Urban areas with the appropriate thermal environment attract people. The outer thermal environment is divided into air temperature, wind speed, relative humidity, and mean radiant temperature. This research paper analyzed several mitigation strategies using simulation software, which will help in modifying the urban areas. According to the results within the studied area, the addition of vegetation is significantly effective on the thermal environment, followed by the cool pavement and by the replacement of old building with new ones.

Vegetation blocks the short-wave radiation and reduces the air temperature by transpiration. Increasing the vegetation cover would help and protect the pedestrian from direct sunshine, thus reduce the mean radiant temperature and improve thermal comfort based on the results.

Also, another factor which reduces due to shading produced is the longwave radiation. It leads to a decrease in the ground surface temperature. Replacing old buildings with new ones by changing the materials of the buildings, show a small change in the mean radiant temperature near the new buildings because of the different materials that have different densities, thermal conductivity, and specific heat capacity. Using reflective surfaces such as cool pavement with higher albedo fraction absorbs less solar radiation, and therefore has a lower surface temperature. Absorbing less solar radiation means that the cool pavement emits less longwave radiation, and the air temperature is as a result lower. Finally, a comparison of the combined cases, including the three proposed strategies, revealed the greatest effect on mitigating the UHI in the summer. These results support other results from previous studies, which also validated the same results.

In conclusion, this study provides important guidelines for landscape architects and urban planners. It identifies the significant benefits that can result in increasing vegetation in urban

areas and can help inform planning and design guidelines applicable to the city and buildings. It can be applied to other sites in parallel with Beirut's climate. Also, it is necessary to find ways in urban planning to mitigate the adverse effects of global warming in the Mediterranean cities, and urban vegetation should be considered as an additional guideline in mitigation strategies for outdoor spaces.

Further investigation is needed to integrate the pollution scuttle in assessing mitigation strategies. Future studies should consider the following point of view such as the building cooling energy after adding vegetation, trying to add different type of trees, and adding vegetation at the roof top. Moreover, field measurements should be conducted to evaluate the simulated output data and should include validation of the study by applying those strategies on other case studies in Beirut. However, anthropogenic heat release and car transportation heat fluxes were not taken into account by ENVI-met software and were considered as limitations.

BIBLIOGRAPHY

- (2018). Retrieved from Greenspec: <https://www.greenspec.co.uk/building-design/thermal-mass/>
- Aboelata, A., & Sodoudi, S. (2019). *Evaluating urban vegetation scenarios to mitigate urban heat island and reduce buildings' energy in dense built-up areas in Cairo. Building and Environment, 166*, 106407.
- Akbari, H., Pomerantz, M., Taha, H. (2001). Cool surfaces and shade trees to reduce energy use and improve air quality in urban areas. *Sol. Energy, Urban Environment 70*, 295–310.
- Ali-Toudert, F., & Mayer, H. . (2006). Numerical study on the effects of aspect ratio and orientation of an urban street canyon on outdoor thermal comfort in hot and dry climate. *Building and environment, 41(2)*, 94-108.
- Alonso, M. S., Labajo, J. L., & Fidalgo, M. R. . (2003). Characteristics of the urban heat island in the city of Salamanca, Spain. *Atmósfera, 16(3)*, 137-148.
- Asaeda, A., Ca, V.T., Akio Wake, A. (1994). Heat storage of pavement and its effect on the lower atmosphere, *Atmospheric environment, Vol. 30, No. 33*, pp. 413-427.
- ASHRAE. (2009). 2009 ASHRAE handbook, Fundamentals. 1st Edn., ASHRAE, Atlanta, GA., ISBN: 9781615830015.
- Bowler, D.E., Buyung-Ali, L., Knight, T.M., Pullin, A.S. (2010). Urban greening to cool towns and cities: A systematic review of the empirical evidence. *Landsc. Urban Plan. 97*, 147–155.
- Bruse, M. (2016). <http://www.envi-met.com>.
- Chatzidimitriou, A., & Axarli, K. . (2017). Street canyon geometry effects on microclimate and comfort: A case study in thessaloniki. *Procedia Environ. Sci, 38*, 643-650.
- Che-Ani, A. I., Shahmohamadi, P., Sairi, A., Mohd-Nor, M. F. I., Zain, M. F. M., & Surat, M. (2009). Mitigating the urban heat island effect: Some points without altering existing city planning. *European Journal of Scientific Research, 35(2)*, 204-216.
- Dimoudi, A., Zoras, S., Kantzioura, A., Stogiannou, X., Kosmopoulos, P., & Pallas, C. . (2014). Use of cool materials and other bioclimatic interventions in outdoor places in order to mitigate the urban heat island in a medium size city in Greece. *Sustainable Cities and Society, 13*, 89-96.
- Doulos, L., Santamouris, M., & Livada, I. . (2004). Passive cooling of outdoor urban spaces. The role of materials. *Solar energy, 77(2)*, 231-249.
- Eichelberger et. al. (2008). Climate change effects on wind speed. *North American Windpower, 7*, 68-72.
- Evapotranspiration: The Oft-Forgotten Outflow*. (2012). Retrieved from <https://balancingthebasin.armylive.dodlive.mil/2012/12/10/evapotranspiration-the-oft-forgotten-outflow/>
- Gartland, L. M. . (2012). *Heat islands: understanding and mitigating heat in urban areas*. Routledge.
- Gaspari, J., & Fabbri, K. . (2017). A study on the use of outdoor microclimate map to address design solutions for urban regeneration. *Energy Procedia, 111*, 500-509.

- Gasparrini, A., Guo, Y., Sera, F., Vicedo-Cabrera, A. M., Huber, V., Tong, S., ... & Ortega, N. V. . (2017). Projections of temperature-related excess mortality under climate change scenarios. *The Lancet Planetary Health*, 1(9), e360-e367.
- Giannopoulou, K., Livada, I., Santamouris, M., Saliari, M., Assimakopoulos, M., & Caouris, Y. G. . (2011). On the characteristics of the summer urban heat island in Athens, Greece. *Sustainable Cities and Society*, 1(1), 16-28.
- Givoni, B., Noguchi, M., Saaroni, H., Pochter, O., Yaacov, Y., Feller, N., & Becker, S. (2003). Outdoor comfort research issues. *Energy and buildings*, 35(1), 77-86.
- Google Earth. (2017).
- Grimmond, C. S. B., & Oke, T. R. . (1991). An evapotranspiration-interception model for urban areas. *Water Resources Research*, 27(7), 1739-1755.
- Heat Island*. (n.d.). Retrieved from <https://heatisland.lbl.gov/>
- Jaafar, H., Lakkis, I., Yeretian, A. (2020). The Effect of Trees on Urban Microclimate and Outdoor Thermal Comfort in the City of Beirut: A Model-Based Study. *Submitted to ASHRAE Conference 2020*.
- Jansson, Å. (2013). Reaching for a sustainable, resilient urban future using the lens of ecosystem services. *Ecological Economics*, 86, 285-291.
- Kaloustian, N., & Diab, Y. . (2015). Effects of urbanization on the urban heat island in Beirut. *Urban Climate*, 14, 154-165.
- Kamal-Chaoui, L., & Robert, A. . (2009). Competitive cities and climate change.
- Kleerekoper, L., Van Esch, M., & Salcedo, T. B. . (2012). How to make a city climate-proof, addressing the urban heat island effect. *Resources, Conservation and Recycling*, 64, 30-38.
- Köppen, W. . (1990). Versuch einer Klassifikation der Klimate, vorzugsweise nach ihren Beziehungen zur Pflanzenwelt. *Geographische Zeitschrift*, 6(11. H), 593-611.
- Kourtidis, K., Georgoulas, A. K., Rapsomanikis, S., Amiridis, V., Keramitsoglou, I., Hooyberghs, H., ... & Melas, D. . (2015). A study of the hourly variability of the urban heat island effect in the Greater Athens Area during summer. *Science of the Total Environment*, 517, 162-177.
- Lee, H., Mayer, H., Chen, L. (2016). Contribution of trees and grasslands to the mitigation of human heat stress in a residential district of Freiburg, Southwest Germany. *Landsc. Urban Plan.* 148, 37–50.
- Lindberg, F., Holmer, B., & Thorsson, S. . (2008). SOLWEIG 1.0—Modelling spatial variations of 3D radiant fluxes and mean radiant temperature in complex urban settings. *International journal of biometeorology*, 52(7), 697-713.
- Loughner, C. P., Allen, D. J., Zhang, D. L., Pickering, K. E., Dickerson, R. R., & Landry, L. . (2012). Roles of urban tree canopy and buildings in urban heat island effects: Parameterization and preliminary results. *Journal of Applied Meteorology and Climatology*, 51(10), 1775-1793.
- Middel, A., Häb, K., Brazel, A.J., Martin, C.A., Guhathakurta, S. (2014). Impact of urban form and design on mid-afternoon microclimate in Phoenix Local Climate Zones. *Landsc. Urban Plan.* 122, 16–28.

- Nasir, R. A., Ahmad, S. S., Zain-Ahmed, A., & Ibrahim, N. . (2015). Adapting Human Comfort in an Urban Area: The role of tree shades towards urban regeneration. *Procedia-Social and Behavioral Sciences*, 170, 369-380.
- O'Malley, C., Piroozfar, P., Farr, E. R., & Pomponi, F. . (2015). Urban Heat Island (UHI) mitigating strategies: A case-based comparative analysis. *Sustainable Cities and Society*, 19, 222-235.
- Oke, T. R. . (2002). *Boundary layer climates*. Routledge.
- Pachauri, R. K., Allen, M. R., Barros, V. R., Broome, J., Cramer, W., Christ, R., ... & Dubash, N. K. . (2014). *Climate change 2014: synthesis report. Contribution of Working Groups I, II and III to the fifth assessment report of the Intergovernmental Panel on Climate Change* (p. 151). *Ipcc*.
- Peri, G., Rizzo, G., Scaccianoce, G., La Gennusa, M., & Jones, P. . (2016). Vegetation and soil-related parameters for computing solar radiation exchanges within green roofs: Are the available values adequate for an easy modeling of their thermal behavior?. *Energy and Buildings*, 129, 535-548.
- Santamouris, M. (2013). *Energy and climate in the urban built environment*. Routledge.
- Santamouris, M. . (2014). Cooling the cities—a review of reflective and green roof mitigation technologies to fight heat island and improve comfort in urban environments. *Solar energy*, 103, 682-703.
- Santamouris, M., Gaitani, N., Spanou, A., Saliari, M., Giannopoulou, K., Vasilakopoulou, K., & Kardomateas, T. . (2012). Using cool paving materials to improve microclimate of urban areas—Design realization and results of the flisvos project. *Building and Environment*, 53, 128-136.
- Santamouris, M., Synnefa, A., & Karlessi, T. (2011). Using advanced cool materials in the urban built environment to mitigate heat islands and improve thermal comfort conditions. *Solar Energy*, 85(12), 3085-3102.
- Simon, H. (2016). *Development, implementation and evaluation of new and improved calculation methods for the urban microclimate model ENVI-met* (Doctoral dissertation, Ph. D. thesis, Fachbereich Chemie, Pharmazie und Geowissenschaften der Johannes Gutenberg-Universität Main).
- Synnefa, A., Dandou, A., Santamouris, M., Tombrou, M., & Soulakellis, N. . (2008). On the use of cool materials as a heat island mitigation strategy. *Journal of Applied Meteorology and Climatology*, 47(11), 2846-2856.
- Synnefa, A., Santamouris, M., & Livada, I. . (2006). A study of the thermal performance of reflective coatings for the urban environment. *Solar Energy*, 80(8), 968-981.
- Taha, H., . (1997). Urban climates and heat islands: albedo, evapotranspiration, and anthropogenic heat. *Energy and Buildings* 25, 99–103.
- Takebayashi, H., & Moriyama, M. . (2012). Relationships between the properties of an urban street canyon and its radiant environment: Introduction of appropriate urban heat island mitigation technologies. *Solar Energy*, 86(9), 2255-2262.
- Tsilini, V., Papantoniou, S., Kolokotsa, D. D., & Maria, E. A. . (2015). Urban gardens as a solution to energy poverty and urban heat island. *Sustainable cities and society*, 14, 323-333.

- UN 2015 United Nation Population Division*. (2015). Retrieved from data.un.org/CountryProfile.aspx/_Docs/CountryProfile.aspx?crName=Lebanon
- Wang, Y., & Akbari, H. . (2016). Analysis of urban heat island phenomenon and mitigation solutions evaluation for Montreal. *Sustainable Cities and Society*, 26, 438-446.
- Weng, Q. . (2001). A remote sensing? GIS evaluation of urban expansion and its impact on surface temperature in the Zhujiang Delta, China. *International journal of remote sensing*, 22(10), 1999-2014.
- Zinzi, M., & Agnoli, S. . (2012). Cool and green roofs. An energy and comfort comparison between passive cooling and mitigation urban heat island techniques for residential buildings in the Mediterranean region. *Energy and Buildings*, 55, 66-76.